

The ℓ_1 -Constrained Minimal Singular Value: a Computable Quantification of the Stability of Sparse Signal Reconstruction

Gongguo Tang and Arye Nehorai

Department of Electrical and Systems Engineering

Washington University in St. Louis

St. Louis, MO 63130-1127

Email: nehorai@ese.wustl.edu

Abstract

The stability of sparse signal reconstruction is investigated in this paper. The ℓ_1 -constrained minimal singular value (ℓ_1 -CMSV) of the measurement matrix is shown to determine, in a very concise manner, the reconstruction performance of ℓ_1 -based algorithms such as Basis Pursuit, the Dantzig selector, and the LASSO estimator. Compared with performance analysis involving the Restricted Isometry Property, the arguments in this paper are much less complicated and provide more intuition on the stability of sparse signal recovery. Numerical simulations show that the ℓ_1 -CMSV based bounds are tighter and apply to sensing matrix with a wider range of sizes. We show also that, with high probability, the Bernoulli ensemble and a modified Fourier ensemble generate measurement matrices with ℓ_1 -CMSVs bounded away from zero, as long as the number of measurements is relatively large. Another major advantage of using the ℓ_1 -CMSV instead of the Restricted Isometry Constant to quantify reconstruction performance is computational. To compute the ℓ_1 -CMSV, three algorithms based on projected gradient method and interior point algorithm are developed. A lower bound of the ℓ_1 -CMSV is also available by solving a semi-definite programming problem obtained via the lifting procedure.

This work was supported by the Department of Defense under the Air Force Office of Scientific Research MURI Grant FA9550-05-1-0443, and ONR Grant N000140810849.

Index Terms

ℓ_1 -constrained minimal singular value, Basis Pursuit, Dantzig selector, interior point algorithm, LASSO estimator, projected gradient method, restricted isometry property, sparse signal reconstruction, semidefinite relaxation

I. INTRODUCTION

Sparse signal reconstruction aims at recovering a sparse signal $\mathbf{x} \in \mathbb{R}^n$ from observations of the following model:

$$\mathbf{y} = A\mathbf{x} + \mathbf{w}, \quad (1)$$

where $A \in \mathbb{R}^{m \times n}$ is the measurement or sensing matrix, \mathbf{y} is the measurement vector, and $\mathbf{w} \in \mathbb{R}^m$ is the noise vector. The sparsity level k of \mathbf{x} is defined as the number of non-zero components of \mathbf{x} . The measurement system is underdetermined because the number of measurements m is much less than the signal dimension n . However, when the sparsity level k is also very small, it is possible to recover \mathbf{x} from \mathbf{y} in a stable manner. Reconstruction of a sparse signal from noisy linear measurements appears in many signal processing branches, such as compressive sensing [1]–[3], sparse linear regression [4], source localization [5], [6], sparse approximation, and signal denoising [7]. Model (1) is applicable to many practical areas, for example, DNA microarrays [8]–[11], radar imaging [12]–[14], cognitive radio [15], and sensor arrays [5], [6], to name a few.

This paper is motivated by the following considerations. When we are given a sensing or measurement system (1), we usually want to know the performance of the system before using it. This involves deriving a performance measure which is computable, given the sensing matrix A as well as the signal and noise structures. Furthermore, in signal processing and the applications mentioned in the previous paragraph, we usually have the freedom to design the sensing matrix; that is, we can choose the best from a collection of sensing matrices. For example, in radar imaging and sensor array applications, sensing matrix design is connected with waveform design and array configuration design. To optimally design the sensing matrix, we need to

- 1) analyze how the performance of recovering \mathbf{x} from \mathbf{y} is affected by A , and define a function $\rho(A)$ to accurately quantify the goodness of A in the context of sparse signal reconstruction;

- 2) develop algorithms to efficiently compute $\rho(A)$ for arbitrary given A ;
- 3) design mechanisms to select within a matrix class the sensing matrix that is optimal in the sense of best $\rho(A)$.

There is a copious literature, which we will discuss later, on the first aspect but not much on the second and the third. According to the literature, the goodness of A is its incoherence property measured by, most notably, the Restricted Isometry Constant (RIC). Unfortunately, for a given arbitrary matrix, the RIC is extremely difficult to compute, if not impossible. So a stochastic framework is usually adopted to argue that the majority of a certain class of randomly generated matrices have good RICs. However, this framework is not satisfactory, considering our three-step scheme for optimal design. As a consequence, the remaining two steps in designing an optimal sensing matrix using RIC are nearly hopeless.

There are other computationally trivial coherence measures, such as mutual coherence, which is defined as the maximal inner product between the columns of A [16]. Some work addresses the optimal sensing matrix design problem using mutual coherence. For example, Elad [17] proposes an iterative algorithm using shrinkage to minimize an appropriately averaged version of mutual coherence. In [18] Duarte-Carvajalino and Sapiro approach the problem by making the Gram matrix $A^T A$ as close to the identity matrix as possible. Both approaches are inspiring, and their optimized sensing matrices exhibit improved reconstruction performance compared with randomly generated ones. However, mutual incoherence does not produce an accurate bound on the reconstruction error. This paper investigates the possibility of finding a good measure $\rho(A)$ to fulfill step 1) and possibly step 2). We will not consider step 3) in this paper.

We review several approaches to obtain \mathbf{x} from its measurements \mathbf{y} . In a noiseless setting, a natural strategy to recover the true \mathbf{x} is to find the sparsest solution that is consistent with the measurement, *i.e.*,

$$\min \|\boldsymbol{\theta}\|_0 \quad \text{subject to} \quad \mathbf{y} = A\boldsymbol{\theta}, \quad (2)$$

where $\|\cdot\|_0$ counts the number of non-zero components of $\boldsymbol{\theta}$. Unfortunately, the optimization problem (2) is NP-hard. A variety of computationally affordable methods, which work well for the noisy case, are proposed to estimate $\boldsymbol{\theta}$ by exploiting its sparsity structure. These methods can be roughly classified into two categories: iterative methods and convex relaxations. Iterative methods, such as orthogonal matching pursuit [19], CoSaMP [20], subspace pursuit [21], LARS

[22], and so on, obtain the sparse vector θ by alternately estimating the support for θ and the component values. Convex relaxation based methods replace the ℓ_0 norm in (2) with other sparsity-enforcing but convex functions of θ , such as the ℓ_1 norm. Examples of convex relaxation methods include Basis Pursuit [23], the Dantzig selector [24], the LASSO estimator [25], etc. The performance of these algorithms are analyzed in terms of, for example, upper bounds on ℓ_1 and ℓ_2 norms of the estimation errors [19]–[21], [24]. An alternative performance measure is the probability of error in support recovery. In this case, several universal lower bounds on the probability of error are derived for different model assumptions [26], [27]. In this paper, we will focus on convex relaxation algorithms and their reconstruction stability, as measured by bounds on the ℓ_2 norm of estimation errors.

Many conditions on the sensing matrix A have been proposed to guarantee a stable signal reconstruction, most notably the Restricted Isometry Property (RIP) [1], [28] and the Null Space Property (NSP) [29]. Unfortunately, these conditions are extremely expensive to compute. Therefore, various bounds on quantities involved in the RIP and the NSP are computed using, for example, semi-definite programming [30], [31]. We will show that the stability of several popular convex relaxation algorithms, for example, Basis Pursuit [23], the Dantzig selector [24], and the LASSO estimator [25], [32], whose performance analysis motivates the RIP, can be guaranteed by much simpler conditions. These conditions involve a quantity of the sensing matrix we define as the ℓ_1 -CMSV. Interestingly, the ℓ_1 -CMSV is closely related to sparse principal component analysis [30], [33].

The contribution of the work is threefold. First, we derive concise bounds on the ℓ_2 norm of estimation error for Basis Pursuit, the Dantzig selector, and the LASSO estimator. These bounds are concisely related to the ℓ_1 -CMSV. Although one can always express the bounds based on RIC in simple forms by reparametrization, the reparametrization is not universal because it is problem specific. In addition, after reparameterization, the RIC loses its intuitive meaning as a measure of orthogonality of the sensing matrix applied to sparse vectors. Compared with derivations using the RIP condition, the arguments are clearer and more intuitive. There are basically two steps. We first establish that the error vector $\mathbf{h} = \hat{\mathbf{x}} - \mathbf{x}$, with $\hat{\mathbf{x}}$ the estimate of \mathbf{x} , is sparse in the sense that the ratio of its ℓ_1 norm to its ℓ_2 norm is bounded away from \sqrt{n} . We discuss why this ratio is a measure of sparsity in Section III. We then show that given the sparsity of \mathbf{h} the ℓ_2 norm of $A\mathbf{h}$ is both lower bounded and upper bounded, where the lower bound involves the

ℓ_1 -CMSV of A . Second, we demonstrate that if the number of measurements m is reasonably large, random matrices with Bernoulli distributed entries have ℓ_1 -CMSVs bounded away from zero, with high probability. The lower bound on m is not as good as the bound for the RIP, but better techniques can improve it. Last but not least, we develop algorithms to compute the ℓ_1 -CMSV for an arbitrary sensing matrix and compare their performance. These algorithms are by no means the most efficient ones. Once we shift from an optimization problem with a discrete nature (*e.g.*, the RIC) to a continuous one, there are many optimization tools available and more efficient algorithms can be designed.

The paper is organized as follows. In Section II, we present our measurement model, three convex relaxation algorithms, and the RIP condition. Section III is devoted to deriving bounds on the errors of several convex relaxation algorithms. In Section IV, we show that the majority of realizations of the Bernoulli measurement ensemble have good ℓ_1 -CMSVs. In Section V, we design algorithms to compute the ℓ_1 -CMSV and the lower bound on it. We compare the algorithms' performance in Section VI. Section VII summarizes our conclusions.

II. THE MEASUREMENT MODEL, RECONSTRUCTION ALGORITHMS, AND RESTRICTED ISOMETRY PROPERTY

A. The Measurement Model

The following measurement model is used throughout the paper. Suppose we have a sparse signal $\mathbf{x} \in \mathbb{R}^n$, *i.e.*, \mathbf{x} has only a few non-zero components. The sparsity level k of \mathbf{x} is defined as the number of non-zero elements of \mathbf{x} , or put in another way, the ℓ_0 norm of \mathbf{x} : $k = \|\mathbf{x}\|_0$. We call a vector k -sparse if its sparsity level $\|\mathbf{x}\|_0 \leq k$.

We observe $\mathbf{y} \in \mathbb{R}^m$ through the following linear model:

$$\mathbf{y} = A\mathbf{x} + \mathbf{w}, \tag{3}$$

where $A \in \mathbb{R}^{m \times n}$ is the sensing/measurement matrix and $\mathbf{w} \in \mathbb{R}^m$ is the noise/disturbance vector, either deterministic or random. In the deterministic setting we assume boundedness: $\|\mathbf{w}\|_2 \leq \epsilon$, while in the stochastic setting we assume Gaussianity: $\mathbf{w} \sim \mathcal{N}(0, \sigma^2 \mathbf{I}_m)$. The sensing model (3) is generally underdetermined with $m \ll n$, and the sparsity level k is very small.

A fundamental problem pertaining to model (3) is to reconstruct the signal \mathbf{x} from the measurement \mathbf{y} by exploiting sparsity as well as the stability of the reconstruction with respect

to noise. For any reconstruction algorithm, we denote the estimate of \mathbf{x} as $\hat{\mathbf{x}}$, and the error vector $\mathbf{h} \stackrel{\text{def}}{=} \hat{\mathbf{x}} - \mathbf{x}$. In this paper, the stability problem aims to bound $\|\mathbf{h}\|_2$ in terms of m, n, k , the sensing matrix A , and the noise strength ϵ or σ^2 .

B. Reconstruction Algorithms

We briefly review three reconstruction algorithms based on convex relaxation: Basis Pursuit, the Dantzig selector, and the LASSO estimator. A common theme of these algorithms is enforcing the sparsity of solutions by penalizing large ℓ_1 norms. As a relaxation of the ℓ_0 norm, the ℓ_1 norm remains a measure of sparsity while being a convex function. Most computational advantages of the aforementioned three algorithms result from the convexity of the ℓ_1 norm. As demonstrated in Section III, the ℓ_1 sparsity enforcement guarantees sparsity of the error vector in the sense made precise in Section III.

The Basis Pursuit algorithm [23] tries to minimize the ℓ_1 norm of solutions subject to the measurement constraint. It is applicable to both noiseless settings and bounded noise settings with a known noise bound ϵ . The Basis Pursuit algorithm was originally developed for the noise-free case, i.e., $\epsilon = 0$ in (4). In this paper, we refer to both cases as Basis Pursuit. Mathematically, Basis Pursuit solves:

$$\text{BP : } \min_{\mathbf{z} \in \mathbb{R}^n} \|\mathbf{z}\|_1 \quad \text{subject to} \quad \|\mathbf{y} - A\mathbf{z}\|_2 \leq \epsilon. \quad (4)$$

In the context of sparse approximation, Basis Pursuit avoids overfitting by selecting a parsimonious representation within a specified approximation error limit. When $\epsilon = 0$, the optimization problem (4) can be rewritten as a linear program by setting $\mathbf{z} = \mathbf{z}^+ - \mathbf{z}^-$:

$$\begin{aligned} & \min_{\mathbf{z}^+, \mathbf{z}^- \in \mathbb{R}^n} \begin{bmatrix} \mathbf{1}_n^T & \mathbf{1}_n^T \end{bmatrix} \begin{bmatrix} \mathbf{z}^+ \\ \mathbf{z}^- \end{bmatrix} \\ & \text{subject to} \\ & \begin{bmatrix} A & -A \end{bmatrix} \begin{bmatrix} \mathbf{z}^+ \\ \mathbf{z}^- \end{bmatrix} = \mathbf{y}, \\ & \mathbf{z}^+ \geq 0, \quad \mathbf{z}^- \geq 0. \end{aligned} \quad (5)$$

Here $\mathbf{1}_n \in \mathbb{R}^n$ is the column vector of all ones. For $\epsilon > 0$, (4) still falls into the category of convex programming.

The Dantzig selector [24] aims to reconstruct a reasonable signal in most cases when the measurement is contaminated by unbounded noise. Its estimate for \mathbf{x} is the solution to the ℓ_1 -regularization problem:

$$\text{DS : } \quad \min_{\mathbf{z} \in \mathbb{R}^n} \|\mathbf{z}\|_1 \quad \text{subject to} \quad \|A^T \mathbf{r}\|_\infty \leq \lambda_n \cdot \sigma, \quad (6)$$

where $\mathbf{r} = \mathbf{y} - A\mathbf{z}$ is the residual vector, σ the noise standard deviation, and λ_n a control parameter. The constraint $\|A^T \mathbf{r}\|_\infty \leq \lambda_n \cdot \sigma$ requires that all feasible solutions must have uniformly bounded correlations between the induced residual vector and the columns of the sensing matrix. One motivation behind this constraint is to include in the solution variables that are highly correlated with the observation \mathbf{y} . Refer to [24] for discussions on reasons of controlling the size of the correlated residual vector rather than the size of the residual itself as in Basis Pursuit. We emphasize that the optimization problem (DS) is convex and can be cast as a linear program [24]:

$$\begin{aligned} & \min_{\mathbf{u}, \mathbf{z} \in \mathbb{R}^n} \sum_i \mathbf{u}_i \\ & \text{subject to} \\ & -\mathbf{u} \leq \mathbf{z} \leq \mathbf{u} \\ & -\lambda_n \sigma \mathbf{1}_n \leq A^T(\mathbf{y} - A\mathbf{z}) \leq \lambda_n \sigma \mathbf{1}_n. \end{aligned} \quad (7)$$

The LASSO estimator, as originally introduced, solved the optimization problem [25]:

$$\min_{\mathbf{z} \in \mathbb{R}^n} \frac{1}{2} \|\mathbf{y} - A\mathbf{z}\|_2^2 \quad \text{subject to} \quad \|\mathbf{z}\|_1 \leq t, \quad (8)$$

for some $t > 0$. Following the convention in [32], in this paper we refer to the solution to the following closely related optimization problem as the LASSO estimator:

$$\text{LASSO: } \quad \min_{\mathbf{z} \in \mathbb{R}^n} \|\mathbf{y} - A\mathbf{z}\|_2^2 + \lambda_n \|\mathbf{z}\|_1. \quad (9)$$

The optimization problems (8) and (9) are equivalent in the sense that given $t \geq 0$, there exists a $\lambda_n \geq 0$ such that the two problems have the same solution, and vice versa [34]. Problem (8) is usually referred to as constrained regression, while problem (9) is ℓ_1 -penalized regression. The latter (with a $\frac{1}{2}$ factor before the first term) is also called basis pursuit denoising (BPDN) in [35], which proposed a primal-dual log-barrier algorithm to solve it.

C. Restricted Isometry Property

In this section, we present stability results related to Basis Pursuit, the Dantzig selector, and the LASSO estimator. We saw in the previous section that all three optimizations can be implemented using convex programming or even linear programming. The aim of stability analysis is to derive error bounds of the solutions of these algorithms. These bounds usually involve the incoherence of the sensing matrix A , which is measured by the RIC defined below [3], [28]:

Definition 1 For each integer $k \in \{1, \dots, n\}$, the restricted isometry constant (RIC) δ_k of a matrix $A \in \mathbb{R}^{m \times n}$ is defined as the smallest $\delta > 0$ such that

$$1 - \delta \leq \frac{\|A\mathbf{x}\|_2^2}{\|\mathbf{x}\|_2^2} \leq 1 + \delta \quad (10)$$

holds for arbitrary non-zero k -sparse signal \mathbf{x} .

A matrix A with a small δ_k roughly means that A is nearly an isometry when restricted onto all k -sparse vectors. Hence, it is no surprise that the RIC is involved in the stability of recovering \mathbf{x} from $A\mathbf{x}$ corrupted by noise when \mathbf{x} is k -sparse.

The Rayleigh quotient $\frac{\|A\mathbf{x}\|_2^2}{\|\mathbf{x}\|_2^2}$ in the definition of the RIC motivates us to define the k -sparse singular values, which are closely related to the RIC.

Definition 2 For any integer $1 \leq k \leq n$ and matrix $A \in \mathbb{R}^{m \times n}$, define the k -sparse minimal singular value ν_k^{\min} and k -sparse maximal singular value ν_k^{\max} of A via

$$\nu_k^{\min} \stackrel{\text{def}}{=} \min_{\mathbf{x} \neq 0: \|\mathbf{x}\|_0 \leq k} \frac{\|A\mathbf{x}\|_2}{\|\mathbf{x}\|_2}, \quad \text{and} \quad (11)$$

$$\nu_k^{\max} \stackrel{\text{def}}{=} \max_{\mathbf{x} \neq 0: \|\mathbf{x}\|_0 \leq k} \frac{\|A\mathbf{x}\|_2}{\|\mathbf{x}\|_2}, \quad (12)$$

respectively.

When $k = n$, it is easy to see that ν_k^{\min} and ν_k^{\max} are the regular minimal and maximal singular values of A , respectively. The RIC δ_k for matrix A is related to the k -sparse minimal and k -sparse maximal singular values by

$$\delta_k = \max\{1 - (\nu_k^{\min})^2, (\nu_k^{\max})^2 - 1\}. \quad (13)$$

We comment that the computation of δ_k , or ν_k^{\max} and ν_k^{\min} , involves optimizing over the set of all k -sparse signals, which can be divided into $\binom{n}{k}$ subsets with intersections of measure zero

by specifying the exact locations of non-zero components. Consequently, the exact computation of the RIC is extremely difficult.

Now we cite stability results on Basis Pursuit, the Dantzig selector, and the LASSO estimator, which are expressed in terms of the RIC. Assume \mathbf{x} is a k -sparse signal and $\hat{\mathbf{x}}$ is its estimate given by any of the three algorithms; then we have the following:

- 1) Basis Pursuit [28]: Suppose that $\delta_{2k} < \sqrt{2} - 1$ and $\|\mathbf{w}\|_2 \leq \epsilon$. The solution to Basis Pursuit (4) satisfies

$$\|\hat{\mathbf{x}} - \mathbf{x}\|_2 \leq \frac{4\sqrt{1 + \delta_{2k}}}{1 - (1 + \sqrt{2})\delta_{2k}} \cdot \epsilon. \quad (14)$$

- 2) Dantzig selector [24]: Choose $\lambda_n = \sqrt{2 \log n}$ in (6) and assume $\mathbf{w} \sim \mathcal{N}(0, \sigma^2 \mathbf{I}_m)$ and $\delta_{2k} + \delta_{3k} < 1$. Then, with high probability, $\hat{\mathbf{x}}$ obeys

$$\|\hat{\mathbf{x}} - \mathbf{x}\|_2 \leq \frac{4}{1 - \delta_{2k} - \delta_{3k}} \cdot \sqrt{2 \log n} \cdot \sqrt{k} \cdot \sigma. \quad (15)$$

For concreteness, if one chooses $\lambda_n = \sqrt{2(1+t) \log n}$ for each $t > 0$, the bound holds with probability exceeding $1 - \left(\sqrt{\pi(1+t) \log n} \cdot n^t\right)^{-1}$, with $\sqrt{2 \log n}$ replaced by λ_n in (15).

- 3) LASSO estimator [32]: Consider the noise-free case. Under the condition of incoherence design with a sparsity multiplier sequence e_n , the error associated with the LASSO estimator $\hat{\mathbf{x}}$ is bounded for sufficiently large n by

$$\|\hat{\mathbf{x}} - \mathbf{x}\|_2 \leq 17.5 \cdot \lambda_n \cdot \frac{\sqrt{k_n}}{(\nu_{e_n k_n}^{\min})^2}. \quad (16)$$

Here, the sparsity level $k = k_n$ depends on n . Refer to [32] for more information on incoherence design and multiplier sequence.

These results are directly adopted from the given references and are made consistent with our notation. We note the terms involving the RIC on the right hand sides are quite complicated. Their derivations are even more complicated. In addition, the bound for the LASSO estimator requires very technical conditions for its validity. We will compare these results with our bounds in Section III, which are much more concise and whose derivations are much less involved.

Although the RIC provides a measure quantifying the goodness of a sensing matrix, as mentioned earlier, its computation poses great challenge. In the literature, the computation issue is circumvented by resorting to a random argument. We cite one general result below [36]:

- Let $A \in \mathbb{R}^{m \times n}$ be a random matrix whose entries are *i.i.d.* samples from any distribution that satisfies the concentration inequality for any $x \in \mathbb{R}^n$ and $0 < \varepsilon < 1$:

$$\mathbb{P} \left(\left| \|A\mathbf{x}\|_2^2 - \|\mathbf{x}\|_2^2 \right| \geq \varepsilon \|\mathbf{x}\|_2^2 \right) \leq 2e^{-m c_0(\varepsilon)}. \quad (17)$$

Then, for any given $\delta \in (0, 1)$, there exist constants $c_1, c_2 > 0$ depending only on δ such that $\delta_k \leq \delta$, with probability not less than $1 - 2e^{-c_2 m}$, as long as

$$m \geq c_1 k \log \frac{n}{k}. \quad (18)$$

We remark that distributions satisfying the concentration inequality (17) include the Gaussian distribution and the Bernoulli distribution. For the ℓ_1 -CMSV, we will establish a theorem similar to the one above for the Bernoulli ensemble and a modified Fourier ensemble with a slightly worse bound on m .

III. STABILITY OF CONVEX RELAXATION BASED ON THE ℓ_1 -CONSTRAINED MINIMAL SINGULAR VALUE

In this section, we derive bounds on the reconstruction error for the Basis Pursuit, the Dantzig selector and the LASSO estimator. Our bounds are given in terms of the ℓ_1 -CMSV rather than the RIC of matrix A . We first introduce a quantity that measures the sparsity, (or, more accurately, the density), of a given vector \mathbf{x} .

Definition 3 For $p \in (0, 1]$, the ℓ_p -sparsity level of a non-zero vector $\mathbf{x} \in \mathbb{R}^n$ is defined as

$$s_p(\mathbf{x}) = \frac{\|\mathbf{x}\|_p}{\|\mathbf{x}\|_2}, \quad (19)$$

where the ℓ_p semi-norm of \mathbf{x} is $\|\mathbf{x}\|_p = (\sum_{i=1}^n |\mathbf{x}_i|^p)^{1/p}$.

The scaling and permutation invariant $s_p(\mathbf{x})$ is indeed a measure of sparsity. To see this, suppose $\|\mathbf{x}\|_0 = k$; then Hölder's inequality with conjugate pair $\frac{2}{p}$ and $\frac{2}{2-p}$ implies that

$$s_p(\mathbf{x}) \leq k^{\frac{1}{p} - \frac{1}{2}}, \quad (20)$$

and we have equality if and only if the absolute values of all non-zero components of \mathbf{x} are equal. Therefore, the more non-zero elements \mathbf{x} has and the more evenly the magnitudes of these non-zero elements are distributed, the larger $s_p(\mathbf{x})$. In particular, if \mathbf{x} has exactly one non-zero element, then $s_p(\mathbf{x}) = 1$; if \mathbf{x} has n non-zero elements with the same magnitude, then

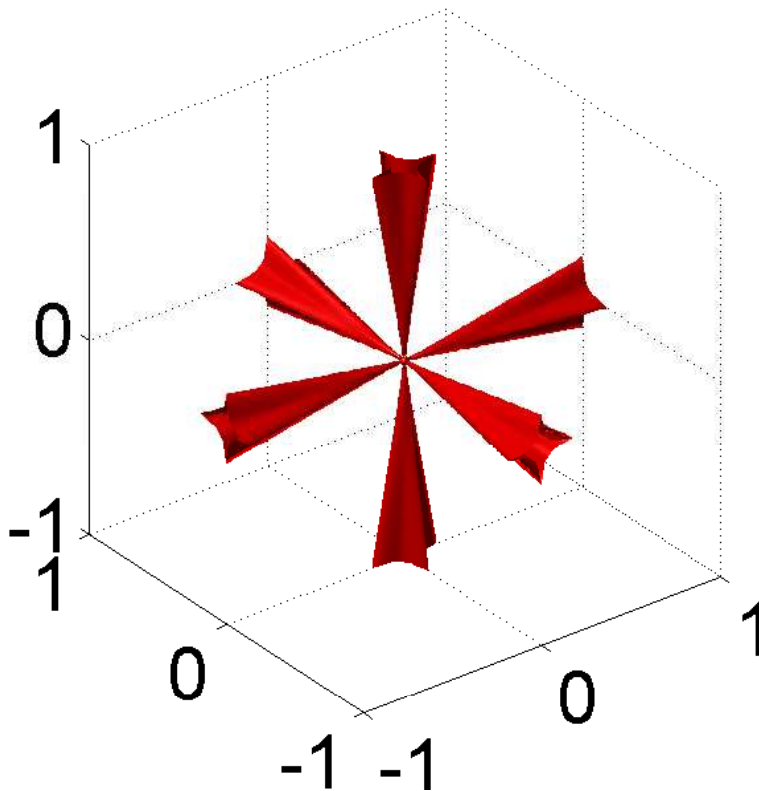


Fig. 1: Regions in \mathbb{R}^3 with $\ell_{1/2}$ -sparsity level 2

$s_p(\mathbf{x}) = n^{1/p-1/2}$. However, if \mathbf{x} has n non-zero elements but their magnitudes are spread in a wide range, then its ℓ_p sparsity level might be very small. We illustrate the set of 3-dimensional vectors $\{\mathbf{x} \in \mathbb{R}^3 : s_p(\mathbf{x}) \leq s\}$ with $p = 1/2$ and $s = 2$ as the region enclosed by the red surface in Figure 1. We can see that when s is small, the vectors concentrate around certain axes, which means the coordinates corresponding to those axes are much larger than the rest of the coordinates. In this paper, we will focus on the ℓ_1 sparsity level $s_1(\mathbf{x})$.

Definition 4 For any $s \in [1, \sqrt{n}]$ and matrix $A \in \mathbb{R}^{m \times n}$, define the ℓ_1 -constrained minimal singular value (abbreviated as ℓ_1 -CMSV) and the ℓ_1 -constrained maximal singular value of A by

$$\rho_s^{\min} \stackrel{\text{def}}{=} \min_{\mathbf{x} \neq 0, s_1(\mathbf{x}) \leq s} \frac{\|A\mathbf{x}\|_2}{\|\mathbf{x}\|_2}, \quad \text{and} \quad (21)$$

$$\rho_s^{\max} \stackrel{\text{def}}{=} \max_{\mathbf{x} \neq 0, s_1(\mathbf{x}) \leq s} \frac{\|A\mathbf{x}\|_2}{\|\mathbf{x}\|_2}, \quad (22)$$

respectively. Because we mainly use ρ_s^{\min} in this paper, for notational simplicity, we sometimes use ρ_s to denote ρ_s^{\min} when it causes no confusion.

Equation (20) implies that $\{\mathbf{x} \neq 0 : \|\mathbf{x}\|_0 \leq k\} \subseteq \{\mathbf{x} \neq 0 : s_1(\mathbf{x}) \leq \sqrt{k}\}$. As a consequence, the sparse singular values satisfy the following inequality

$$\rho_{\sqrt{k}}^{\min} \leq \nu_k^{\min} \leq \nu_k^{\max} \leq \rho_{\sqrt{k}}^{\max}, \quad (23)$$

which combined with (13) yields

$$\delta_k \leq \max \left\{ 1 - (\rho_{\sqrt{k}}^{\min})^2, (\rho_{\sqrt{k}}^{\max})^2 - 1 \right\}. \quad (24)$$

A. Basis Pursuit

In this section, we establish a bound on the ℓ_2 norm of Basis Pursuit's error vector using the ℓ_1 -CMSV. As you will see in the proofs to Theorems 1, 2 and 3, the procedure of establishing these theorems has two steps:

- 1) Show that the error vector $\mathbf{h} = \hat{\mathbf{x}} - \mathbf{x}$ is ℓ_1 -sparse: $s_1(x) \leq 2\sqrt{k}$, which automatically leads to a lower bound $\|\mathbf{A}\mathbf{h}\|_2 \geq \rho_{2\sqrt{k}}\|\mathbf{h}\|_2$;
- 2) Obtain an upper bound on $\|\mathbf{A}\mathbf{h}\|_2$.

For Basis Pursuit (4), the second step is trivial as both \mathbf{x} and $\hat{\mathbf{x}}$ satisfy constraint $\|\mathbf{y} - \mathbf{A}\mathbf{z}\| \leq \epsilon$ in (4). Therefore, the triangle inequality yields

$$\begin{aligned} \|\mathbf{A}\mathbf{h}\|_2 &= \|\mathbf{A}(\hat{\mathbf{x}} - \mathbf{x})\|_2 \\ &\leq \|\mathbf{A}\hat{\mathbf{x}} - \mathbf{y}\|_2 + \|\mathbf{y} - \mathbf{A}\mathbf{x}\|_2 \\ &\leq 2\epsilon. \end{aligned} \quad (25)$$

In order to establish the ℓ_1 -sparsity of the error vector in the first step, we suppose $S = \text{supp}(\mathbf{x})$ and $|S| = \|\mathbf{x}\|_0 = k$. Define the error vector $\mathbf{h} = \hat{\mathbf{x}} - \mathbf{x}$. For any vector $\mathbf{z} \in \mathbb{R}^n$ and any index set $S \subseteq \{1, \dots, n\}$, we use $\mathbf{z}_S \in \mathbb{R}^{|S|}$ to represent the vector whose elements are those of \mathbf{z} indicated by S .

As observed by Candés in [28], the fact that $\|\hat{\mathbf{x}}\|_1 = \|\mathbf{x} + \mathbf{h}\|_1$ is the minimum among all \mathbf{z} satisfying the constraint in (4) implies that $\|\mathbf{h}_{S^c}\|_1$ cannot be very large. To see this, we observe

that

$$\begin{aligned}
\|\mathbf{x}\|_1 &\geq \|\mathbf{x} + \mathbf{h}\|_1 \\
&= \sum_{i \in S} |\mathbf{x}_i + \mathbf{h}_i| + \sum_{i \in S^c} |\mathbf{x}_i + \mathbf{h}_i| \\
&\geq \|\mathbf{x}_S\|_1 - \|\mathbf{h}_S\|_1 + \|\mathbf{h}_{S^c}\|_1 \\
&= \|\mathbf{x}\|_1 - \|\mathbf{h}_S\|_1 + \|\mathbf{h}_{S^c}\|_1.
\end{aligned} \tag{26}$$

Therefore, we obtain $\|\mathbf{h}_{S^c}\|_1 \leq \|\mathbf{h}_S\|_1$, which leads to

$$\begin{aligned}
\|\mathbf{h}\|_1 &= \|\mathbf{h}_S\|_1 + \|\mathbf{h}_{S^c}\|_1 \\
&= 2\|\mathbf{h}_S\|_1 \\
&\leq 2\sqrt{k}\|\mathbf{h}_S\|_2 \\
&\leq 2\sqrt{k}\|\mathbf{h}\|_2,
\end{aligned} \tag{27}$$

where for the next to the last inequality we used the Cauchy-Schwartz inequality. Inequality (27) is equivalent to

$$s_1(\mathbf{h}) \leq 2\sqrt{k}. \tag{28}$$

It follows from (25) and Definition 4 that

$$\rho_{2\sqrt{k}}\|\mathbf{h}\|_2 \leq \|\mathbf{A}\mathbf{h}\|_2 \leq 2\epsilon. \tag{29}$$

Hence, we get

$$\|\hat{\mathbf{x}} - \mathbf{x}\|_2 \leq \frac{2\epsilon}{\rho_{2\sqrt{k}}}. \tag{30}$$

Consequently, we have the following theorem:

Theorem 1 *If the support of \mathbf{x} is of size k and the noise \mathbf{w} is bounded; that is, $\|\mathbf{w}\|_2 \leq \epsilon$, then the solution $\hat{\mathbf{x}}$ to (4) obeys*

$$\|\hat{\mathbf{x}} - \mathbf{x}\|_2 \leq \frac{2\epsilon}{\rho_{2\sqrt{k}}}. \tag{31}$$

Compared with the constant term $\frac{4\sqrt{1+\delta_{2k}}}{1-(1+\sqrt{2})\delta_{2k}}$ in (14), the constant $\frac{2}{\rho_{2\sqrt{k}}}$ here is more concise, and the argument is simpler. In [28], the major effort is devoted to establishing a lower bound on $\|\mathbf{A}\mathbf{h}\|_2$, which is trivial according to Definition 4. Of course, if $\rho_{2\sqrt{k}}$ is not bounded away

from zero, this concise bound will not offer much. We will show in Section IV that, at least for Bernoulli random matrices and modified Fourier matrices, the induced ℓ_1 -CMSVs are bounded away from zero with high probability if m is large enough.

Numerical simulations show that randomly generated matrices are more likely to have $\rho_{2\sqrt{k}}$ bounded away from zero than to have $\delta_{2k} < \sqrt{2} - 1$, the prerequisite for the RIC bound (14) to be applicable. In Figure 2, we plot the RIC δ_{2k} , the ℓ_1 -CMSV $\rho_{2\sqrt{k}}$ computed using the IP II algorithm, and a bound on $\rho_{2\sqrt{k}}$ computed using semidefinite relaxation. Refer to Section V for more details on the algorithm IP II and semidefinite relaxation. Due to the difficulty of computing exact δ_{2k} for large n and k , we select $n = 60$ and $k = 2$. The sensing matrix is a member of the Bernoulli ensemble defined in Definition 5. The RIC is obtained by performing the singular value decomposition for all $m \times k$ submatrices of the Bernoulli matrix. We notice that for $m < n$, which is the region of interest for sparse signal processing, the condition that $\delta_{2k} < \sqrt{2} - 1$ is not satisfied, while when $m \gtrsim 20$, the ℓ_1 -CMSV $\rho_{2\sqrt{k}}$ starts to be greater than 0. As a matter of fact, the RIC δ_{2k} starts to be less than $\sqrt{2} - 1$ only when m is around 300, a value significantly greater than $n = 60$. Therefore, at least for small size Bernoulli matrices, the bound based on ℓ_1 -CMSV in Theorem 1 applies to a wider range of problems than the bound (14) based on RIC.

The ℓ_1 -CMSV bound is also tighter than the RIC bound when both apply as shown in Figure 3. When $\epsilon = 1$, the ℓ_1 -CMSV bound $\frac{2}{\rho_{2\sqrt{k}}}\epsilon$ is approximately 4, while the RIC bound $\frac{4\sqrt{1+\delta_{2k}}}{1-(1+\sqrt{2})\delta_{2k}}\epsilon$ is approximately 30. We would like to make the comparison for $m < n$, but, unfortunately, the RIC based bound is not applicable for n s and k s that the RIC is computable as discussed before. We conclude that, compared with the RIC, the ℓ_1 -CMSV is computationally more amenable, generates more concise and tighter bounds that apply to problems with a wider range of sizes.

B. Dantzig Selector

For simplicity we assume the columns of A are normalized to length 1 as in [24]. Both the Bernoulli matrix and modified Fourier matrix analyzed in Section IV satisfy this condition.

We comment that for the reconstruction problem of (3), if the noise is Gaussian, the results here and in [24] and [32] hold only with high probability. This is reasonable because when the noise is very large, which always happens with a certain probability, we can not expect a controlled error bound independent of the noise realization's magnitude. However, we do not

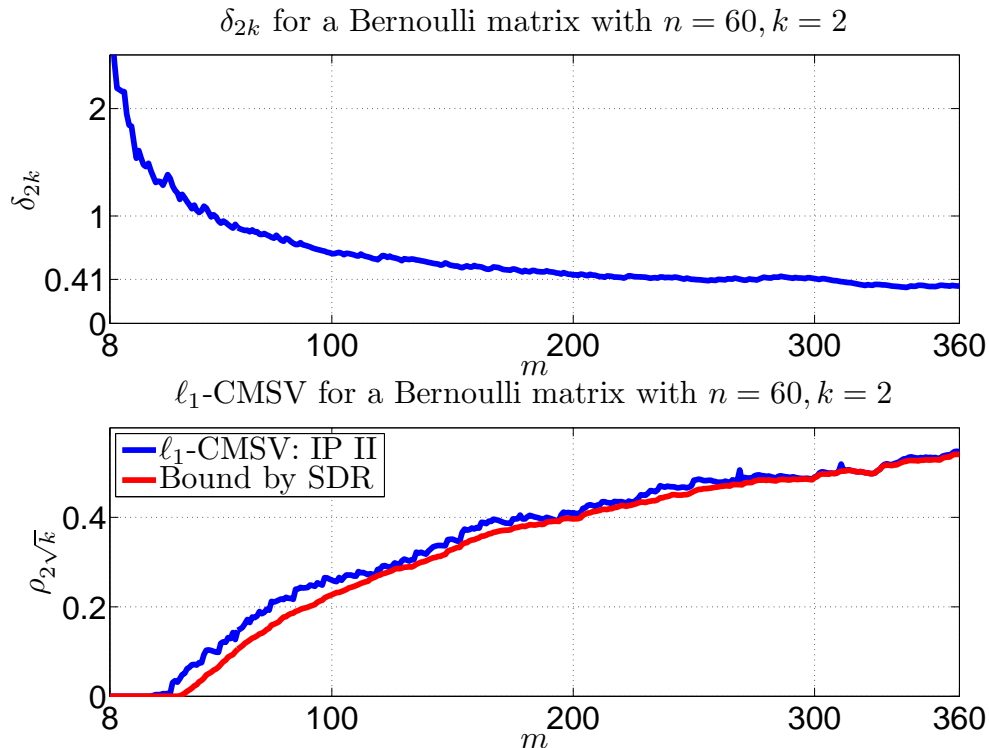


Fig. 2: The RIC δ_{2k} , the ℓ_1 -CMSV $\rho_{2\sqrt{k}}$, and a bound for $\rho_{2\sqrt{k}}$ computed using semidefinite relaxation for a Bernoulli matrix with $n = 60$, $k = 2$, and m ranging from $4k$ to $6n$.

even know if the average error, *i.e.*, the mean squared error $\mathbb{E}(\|\hat{\mathbf{x}} - \mathbf{x}\|_2^2)$, is bounded. In [37], the authors showed that the mean-squared-error for any unbiased estimator of \mathbf{x} is infinite, which justifies the use of biased estimators. As both the Dantzig selector (6) and the LASSO estimator (9) produce biased estimators, we hope the bias-variance tradeoff will lead to a well bounded mean-squared-error.

Hence, before following the road map outlined in Section III-A, we first identify a high probability event E on which the noise is well-behaved. We assume the noise $\mathbf{w} \sim \mathcal{N}(0, \sigma^2 \mathbf{I}_m)$. As shown by Candés and Tao in [24], with high probability, \mathbf{w} satisfies the orthogonality condition

$$|\mathbf{w}^T A_j| \leq \lambda_n \sigma \quad \text{for all } 1 \leq j \leq n, \quad (32)$$

for $\lambda_n = \sqrt{2 \log n}$. More specifically, defining the event

$$E \stackrel{\text{def}}{=} \{\|A^T \mathbf{w}\|_\infty \leq \lambda_n \sigma\}, \quad (33)$$

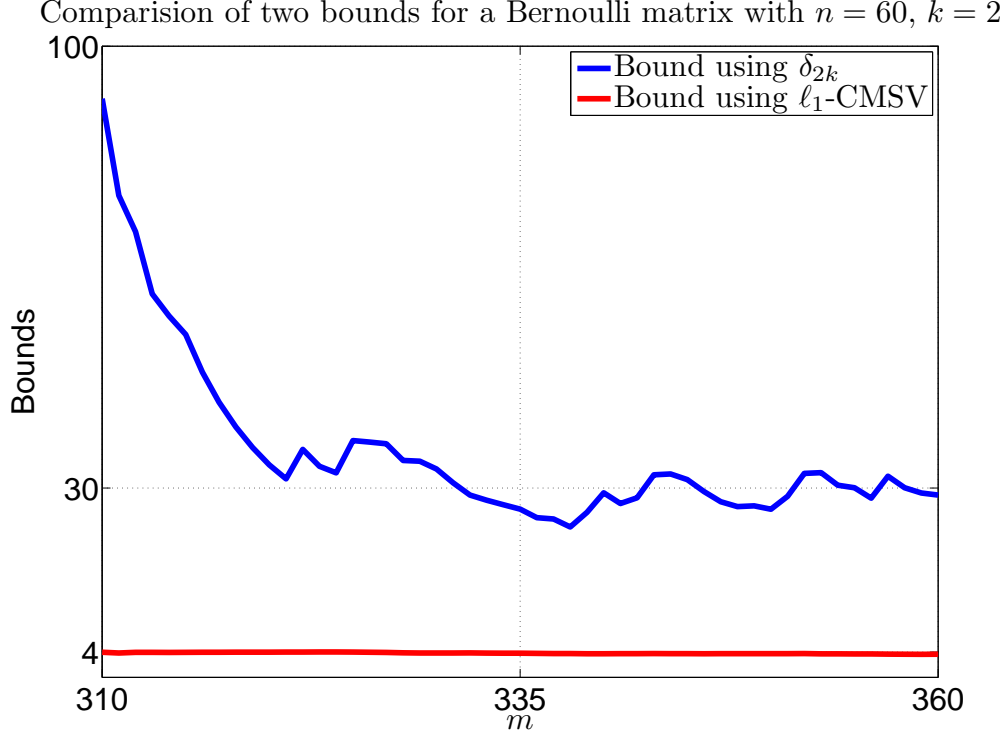


Fig. 3: Comparison of the ℓ_1 -CMSV bound $\frac{2}{\rho_{2\sqrt{k}}}\epsilon$ and the RIC bound $\frac{4\sqrt{1+\delta_{2k}}}{1-(1+\sqrt{2})\delta_{2k}}\epsilon$ for a Bernoulli matrix with $n = 60$, $k = 2$, and $m \in [310, 360]$. Only the constants before ϵ are plotted, *i.e.*, $\epsilon = 1$.

we have

$$\mathbb{P}(E^c) \leq \frac{2n \cdot (2\pi)^{-1/2} e^{-\lambda_n^2/2}}{\lambda_n}. \quad (34)$$

Therefore, with $\lambda_n = \sqrt{2(1+t)\log n}$, we obtain

$$\mathbb{P}(E) \geq 1 - \left(\sqrt{\pi(1+t)\log n} \cdot n^t \right)^{-1}. \quad (35)$$

Hereafter we consider the measurement system (1) and the Dantzig selector (6) under event E .

Suppose $\mathbf{x} \in \mathbb{R}^n$ is a k -sparse signal with support S , and $\hat{\mathbf{x}}$ is the solution to the Dantzig selector (6). Define $\mathbf{h} = \hat{\mathbf{x}} - \mathbf{x}$. We note that to obtain the ℓ_1 -sparsity level result (28), we used only two conditions:

- $\|\hat{\mathbf{x}}\|_1 = \|\mathbf{x} + \mathbf{h}\|_1$ is the minimum among all vector satisfying the optimization constraint;
- the true signal \mathbf{x} satisfies the constraint.

Obviously, the first condition holds simply because of the structure of the Dantzig selector. Conditioned on the event E , the true signal \mathbf{x} also satisfies the constraint:

$$\begin{aligned}\|A^T \mathbf{r}\|_\infty &= \|A^T(\mathbf{y} - A\mathbf{x})\|_\infty \\ &= \|A^T \mathbf{w}\|_\infty \leq \lambda_n \cdot \sigma.\end{aligned}\quad (36)$$

Consequently, we have $s_1(\mathbf{h}) \leq 2\sqrt{k}$, or equivalently,

$$\|\mathbf{h}\|_1 \leq 2\sqrt{k}\|\mathbf{h}\|_2. \quad (37)$$

We now turn to the second step to obtain an upper bound on $\|A\mathbf{h}\|_2$. As shown in [24], on the event E the orthogonality condition (32) and the constraint in the Dantzig selector (6) yield

$$\|A^T A\mathbf{h}\|_\infty \leq 2\lambda_n \sigma \quad (38)$$

as

$$\begin{aligned}A_j^T(\mathbf{w} - \hat{\mathbf{r}}) &= A_j^T[(\mathbf{y} - A\mathbf{x}) - (\mathbf{y} - A\hat{\mathbf{x}})] \\ &= A_j^T(A\hat{\mathbf{x}} - A\mathbf{x}) = A_j^T A\mathbf{h},\end{aligned}\quad (39)$$

where $\hat{\mathbf{r}} = \mathbf{y} - A\hat{\mathbf{x}}$ is the residual corresponding to the Dantzig selector solution $\hat{\mathbf{x}}$. Therefore, we obtain an upper bound on $\|A\mathbf{h}\|_2^2$ as follows:

$$\begin{aligned}\mathbf{h}^T A^T A\mathbf{h} &= \left| \sum_{i=1}^n \mathbf{h}_i (A^T A\mathbf{h})_i \right| \\ &\leq \sum_{i=1}^n |\mathbf{h}_i| \cdot |(A^T A\mathbf{h})_i| \\ &\leq 2\lambda_n \sigma \|\mathbf{h}\|_1.\end{aligned}\quad (40)$$

Equation (40), the definition of $\rho_{2\sqrt{k}}$, and equation (37) together yield

$$\begin{aligned}\rho_{2\sqrt{k}}^2 \|\mathbf{h}\|_2^2 &\leq \mathbf{h}^T A^T A\mathbf{h} \\ &\leq 2\lambda_n \sigma \|\mathbf{h}\|_1 \\ &\leq 4\lambda_n \sqrt{k} \sigma \|\mathbf{h}\|_2.\end{aligned}\quad (41)$$

We conclude that

$$\|\mathbf{h}\|_2 \leq \frac{4}{\rho_{2\sqrt{k}}^2} \cdot \lambda_n \cdot \sqrt{k} \cdot \sigma. \quad (42)$$

Therefore, we have the following theorem:

Theorem 2 Suppose $\mathbf{w} \sim \mathcal{N}(0, \sigma^2 \mathbf{I}_m)$ in the sensing model (3), and suppose $\mathbf{x} \in \mathbb{R}^n$ is a k -sparse signal with support S . Choose $\lambda_n = \sqrt{2 \log n}$ in (6). Then, with high probability, the solution $\hat{\mathbf{x}}$ to (6) satisfies

$$\|\hat{\mathbf{x}} - \mathbf{x}\|_2 \leq \frac{4}{\rho_{2\sqrt{k}}^2} \sqrt{2 \log n} \cdot \sqrt{k} \cdot \sigma. \quad (43)$$

More specifically, if $\lambda_n \stackrel{\text{def}}{=} \sqrt{2(1+t) \log n}$ for each $t \geq 0$, the bound holds with probability greater than $1 - \left(\sqrt{\pi(1+t) \log n} \cdot n^t\right)^{-1}$, with $\sqrt{2 \log n}$ in (43) replaced by λ_n .

Recall that under the same conditions, the result (15) has the constant $\frac{4}{1-\delta_{2k}-\delta_{3k}}$ compared with our constant $\frac{4}{\rho_{2\sqrt{k}}^2}$. These two are not directly comparable, but in a very rough sense $1 - \delta_{2k} - \delta_{3k} \approx 1 - \delta_{5k} \approx (\nu_{5k}^{\min})^2 \approx \rho_{\sqrt{5k}}^2$.

C. LASSO Estimator

We will temporarily drop the subscript n of λ_n for notational simplicity. For the LASSO estimator (9), we can establish a result only for the noise-free case, or the bias of the LASSO estimator as it was termed in [32]. For $0 \leq \xi \leq 1$ we define the de-noised version of the response variable [32] as

$$\mathbf{y}(\xi) = A\mathbf{x} + \xi\mathbf{w}. \quad (44)$$

Correspondingly we define a family of estimators $\hat{\mathbf{x}}^{\lambda, \xi}$ as

$$\hat{\mathbf{x}}^{\lambda, \xi} = \operatorname{argmin}_{\mathbf{z}} \|\mathbf{y}(\xi) - A\mathbf{z}\|_2^2 + \lambda \|\mathbf{z}\|_1. \quad (45)$$

Clearly, we have $\hat{\mathbf{x}}^{\lambda, 1} = \hat{\mathbf{x}}$ as the original LASSO estimator, while $\mathbf{x}^\lambda \stackrel{\text{def}}{=} \hat{\mathbf{x}}^{\lambda, 0}$ is the LASSO estimator in the absence of noise.

Suppose that \mathbf{x} is a k -sparse vector with support S . When there is no noise, we rewrite the LASSO (9) as

$$\min_{\mathbf{z} \in \mathbb{R}^n} \|A\mathbf{z} - A\mathbf{x}\|_2^2 + \lambda \|\mathbf{z}\|_1. \quad (46)$$

Therefore, defining $\mathbf{h} = \mathbf{x}^\lambda - \mathbf{x}$ and $\boldsymbol{\zeta} = \mathbf{z} - \mathbf{x}$, we have

$$\mathbf{h} = \operatorname{argmin}_{\boldsymbol{\zeta} \in \mathbb{R}^n} f(\boldsymbol{\zeta}), \quad (47)$$

where

$$f(\boldsymbol{\zeta}) = \boldsymbol{\zeta}^T A^T A \boldsymbol{\zeta} + \lambda \sum_{i \in S^c} |\zeta_i| + \lambda \sum_{i \in S} |\mathbf{x}_i + \zeta_i| \quad (48)$$

with $S = \text{supp}(\mathbf{x})$. Both steps in the road map of Section III-A rely on the fact that \mathbf{h} achieves the minimum of $f(\boldsymbol{\zeta})$. In particular,

$$f(\mathbf{h}) \leq f(\mathbf{0}) = \lambda \|\mathbf{x}\|_1. \quad (49)$$

Refer to the proof for more details. Following the road map, we show that the bias term $\|\mathbf{x}^\lambda - \mathbf{x}\|_2$ is bounded:

Theorem 3 *Suppose \mathbf{x} is a k -sparse vector with support S . The LASSO estimator \mathbf{x}^λ given by the solution to (9) in the absence of noise obeys*

$$\|\mathbf{x}^\lambda - \mathbf{x}\|_2 \leq \frac{\lambda \sqrt{k}}{\rho_{2\sqrt{k}}^2}. \quad (50)$$

Proof: We first establish the ℓ_1 -sparsity of \mathbf{h} . Note that

$$\begin{aligned} \lambda \|\mathbf{x}\|_1 &= f(\mathbf{0}) \geq f(\mathbf{h}) \\ &= \mathbf{h}^T A^T A \mathbf{h} + \lambda \sum_{i \in S^c} |\mathbf{h}_i| + \lambda \sum_{i \in S} |\mathbf{x}_i + \mathbf{h}_i| \\ &\geq \lambda \|\mathbf{x}\|_1 + \lambda \|\mathbf{h}_{S^c}\|_1 - \lambda \|\mathbf{h}_S\|_1, \end{aligned} \quad (51)$$

since \mathbf{h} achieves the minimum of $f(\boldsymbol{\zeta})$. Therefore, the ℓ_1 norm of \mathbf{h} on S is bounded by its ℓ_1 norm on S^c

$$\|\mathbf{h}_{S^c}\|_1 \leq \|\mathbf{h}_S\|_1. \quad (52)$$

Following the derivation leading to (27), we get the ℓ_1 -sparsity of \mathbf{h} :

$$\|\mathbf{h}\|_2 \leq 2\sqrt{k} \|\mathbf{h}\|_1. \quad (53)$$

Next, we derive an upper bound on $\|A\mathbf{h}\|_2^2$. Again using $f(\mathbf{h}) \leq f(\mathbf{0})$, or equivalently,

$$\begin{aligned} \mathbf{h}^T A^T A \mathbf{h} &\leq -\lambda \|\mathbf{h}_{S^c}\|_1 - \lambda \sum_{i \in S} (|\mathbf{x}_i + \mathbf{h}_i| - |\mathbf{x}_i|) \\ &\leq \lambda \|\mathbf{h}_S\|_1 \\ &\leq \lambda \sqrt{k} \|\mathbf{h}\|_2, \end{aligned} \quad (54)$$

we conclude that

$$\rho_{2\sqrt{k}}^2 \|\mathbf{h}\|_2^2 \leq \mathbf{h}^T A^T A \mathbf{h} \leq \lambda \sqrt{k} \|\mathbf{h}\|_2. \quad (55)$$

Therefore, the conclusion of the theorem holds. \blacksquare

Compared with the bound in (16), the bound in Theorem 3 always holds without complicated conditions such as incoherence design as well as the introduction of sparsity multiplier. Furthermore, it is valid for any finite n .

As illustrated in numerical simulations, the LASSO estimator given by (9) does not lead to the true signal even in the noiseless case. However, if we alter (9) to

$$\min_{\mathbf{z} \in \mathbb{R}^n} \|\mathbf{y} - A\mathbf{z}\|_2 + \lambda_n \|\mathbf{z}\|_1 \quad (56)$$

by removing the square in the first term, then all other arguments hold while (54) becomes

$$\|A\mathbf{h}\|_2 \leq \lambda \sqrt{k} \|\mathbf{h}\|_2. \quad (57)$$

Consequently, using Definition 4 we get

$$\rho_{2\sqrt{k}} \|\mathbf{h}\|_2 \leq \|A\mathbf{h}\|_2 \leq \lambda \sqrt{k} \|\mathbf{h}\|_2, \quad (58)$$

which implies that $\|\mathbf{h}\|_2 = 0$ when

$$\lambda < \frac{\rho_{2\sqrt{k}}}{\sqrt{k}}. \quad (59)$$

The bias is zero for solutions produced by (56) with λ small enough.

IV. ℓ_1 -CONSTRAINED SINGULAR VALUES OF RANDOM MATRICES

This section is devoted to analyzing the property of the ℓ_1 -CMSVs for the Bernoulli ensemble and a modified Fourier ensemble. Although the bounds in Theorem 1, 2 and 3 have concise forms, they are useless if the quantity involved, $\rho_{2\sqrt{k}}$, is zero or approaches zero for most matrices as n, m, k vary in a reasonable manner. We show that, at least for the Bernoulli sensing matrices and modified Fourier sensing matrices, the ℓ_1 -CMSVs are bounded away from zero with high probability. More precisely, we have the following theorem:

Theorem 4 *Given $s \in [1, \sqrt{n}]$, suppose the following condition holds:*

$$m \geq c(\epsilon) s^8 \log n \quad (60)$$

for some constant $c(\epsilon)$ depending on ϵ only. Then, with probability approaching 1 as n approaches infinity, the ℓ_1 -constrained minimal and maximal singular values ρ_s^{\min} and ρ_s^{\max} for a Bernoulli or a modified Fourier sensing matrix $A \in \mathbb{R}^{m \times n}$ defined in Definition 5 and 6, respectively, satisfy

$$|(\rho_s^{\min})^2 - 1| < \epsilon \quad (61)$$

$$|(\rho_s^{\max})^2 - 1| < \epsilon. \quad (62)$$

Recall that for any k -sparsity signal $\mathbf{x} \in \mathbb{R}^n$, its ℓ_1 -sparsity level $s_1(\mathbf{x}) \leq \sqrt{k}$. Hence, considering (24), we obtain a corollary of Theorem 4, that the RIC $\delta_k \leq \epsilon$ with high probability if

$$m \geq c(\epsilon)k^4 \log n. \quad (63)$$

We know that a much better bound $m \geq c(\epsilon)k \log n$ exists in literature [36] for Bernoulli matrices. The best known bound for the Fourier case is $m \geq C(\epsilon)k \log(n) \cdot \log^2(k) \log(k \log(n))$ [38], [39]. We expect to improve the bound (60) in future work by employing better techniques. We also plan to extend Theorem 4 to the Gaussian ensemble and to the original Fourier sensing ensemble. Refer to the discussions following the proof.

The following definitions characterize the Bernoulli sensing ensemble and Fourier sensing ensemble:

Definition 5 A Bernoulli sensing matrix $A = [a_{\alpha,\beta}] \in \mathbb{R}^{m \times n}$ is produced by generating its entries following independent Bernoulli distributions:

$$a_{\alpha,\beta} = \begin{cases} +\frac{1}{\sqrt{m}} & \text{with probability } \frac{1}{2}, \\ -\frac{1}{\sqrt{m}} & \text{with probability } \frac{1}{2}. \end{cases} \quad (64)$$

Definition 6 Denote $W_\alpha = [1, e^{-j\frac{2\pi\alpha}{n}}, \dots, e^{-j\frac{2\pi\alpha(n-1)}{n}}]^T \in \mathbb{C}^n$ with $j = \sqrt{-1}$. A modified Fourier sensing matrix $A = [\mathbf{a}_1^T \dots \mathbf{a}_m^T]^T \in \mathbb{C}^{m \times n}$ is produced by selecting its m rows, with replacement, from $\{W_0/\sqrt{m}, \dots, W_{n-1}/\sqrt{m}\}$:

$$\mathbb{P}\{\mathbf{a}_\alpha = \frac{1}{\sqrt{m}}W_\beta\} = \frac{1}{n}, \quad \beta = 0, \dots, n-1; \quad \alpha = 1, \dots, m. \quad (65)$$

Note that in Definition 6, the generated matrix has exactly m rows with possibly repeated rows. In [40] the Fourier sensing matrix selects each of the n Fourier vectors $\{W_0/\sqrt{m}, \dots, W_{n-1}/\sqrt{m}\}$

with probability $\frac{m}{n}$. Therefore, the size of the resulting matrix is random with approximately m rows in average. It is expected that the behaviors of the two slightly different Fourier ensembles share similar properties in sparse signal reconstruction. Because Theorem 4 will be derived simultaneously for Bernoulli and Fourier ensembles, the notation $\mathbb{F} = \mathbb{R}$ or \mathbb{C} is used for the two cases, respectively.

The proof of Theorem 4 is based on the Pollard bound [41], [42] and an estimate of the covering number of a related set. We introduce here the notion of covering numbers and some background knowledge.

Definition 7 Suppose (\mathcal{X}, d) is a metric space and $C \subseteq \mathcal{X}$. The covering number of C under d , $N(\epsilon, C, d)$, is defined as the smallest number, N , of points $c_1, \dots, c_N \in \mathcal{X}$ such that $C \subseteq \bigcup_{i=1}^N B(c_i, \epsilon)$, where $B(c_i, \epsilon) \stackrel{\text{def}}{=} \{x \in X : d(x, c_i) \leq \epsilon\}$ is a ball centered at c_i with radius ϵ . We call the set $\{c_1, \dots, c_N\}$ an ϵ -cover of C .

We remark that in Definition 7 the points in the ϵ -cover do not necessarily lie in C .

The ϵ -cover forms a good approximation of C in the sense that every point in C is within ϵ distance of some c_i . It is a common technique to prove that some statement holds for points in the ϵ -cover of a set and then to extend that statement to all points in the set. The key step of this argument is to derive a reasonable bound on the covering number. For example, in proving a condition analogous to (60) for the RIC, Barankin used the well-known fact that the covering number for the unit sphere in \mathbb{R}^k is bounded by $(12/\epsilon)^k$ [36]. Unfortunately, the elegant proof in [36] can not be extended trivially to ℓ_1 -CMSVs. The major difficulty is that the set $\{\mathbf{x} \in \mathbb{R}^n : s_1(\mathbf{x}) \leq s\}$ can not be partitioned into subsets which are closed under subtraction, rendering the approximation using ϵ -cover useless. More interested readers are encouraged to check the validity of equation (5.7) in [36]. Therefore, we need to use the covering number technique in a more delicate way, as illustrated in the Pollard bound detailed below.

The Pollard bound characterizes the uniform deviation of average from expectation. The bound is a generalization of the Vapnik-Chervonenkis inequality, a cornerstone of VC theory which covers topics such as VC dimension, structural risk minimization, and support vector machines [42], [43]. Suppose \mathcal{H} is a class of bounded functions defined on $\mathcal{S} \subseteq \mathbb{F}^n$ and $Z_1^m \stackrel{\text{def}}{=} \{\mathbf{z}_1, \dots, \mathbf{z}_m\} \subseteq \mathcal{S}$. The notation $N(\epsilon, \mathcal{H}(Z_1^m), d_1)$ is used to denote the covering number

of

$$\mathcal{H}(Z_1^m) \stackrel{\text{def}}{=} \{(h(\mathbf{z}_1), \dots, h(\mathbf{z}_m))^T \in \mathbb{F}^m : h \in \mathcal{H}\} \quad (66)$$

with d_1 the ℓ_1 metric on \mathbb{F}^m :

$$d_1(\mathbf{x}, \mathbf{y}) = \frac{1}{m} \sum_{i=1}^m |\mathbf{x}_i - \mathbf{y}_i|. \quad (67)$$

The Pollard bound states that for any $m > 1$ and $\epsilon > 0$:

$$\begin{aligned} & \mathbb{P} \left\{ \sup_{h \in \mathcal{H}} \left| \frac{1}{m} \sum_{i=1}^m h(\mathbf{z}_i) - \mathbb{E}\{h(\mathbf{z}_1)\} \right| \geq \epsilon \right\} \\ & \leq 8 \mathbb{E}\{N(\epsilon/8, \mathcal{H}(Z_1^m), d_1)\} e^{-m\epsilon^2/(128M^2)}, \end{aligned} \quad (68)$$

where $Z_1^m = \{\mathbf{z}_1, \dots, \mathbf{z}_m\} \subseteq \mathcal{S}$ are *i.i.d.* samples from a distribution \mathcal{D} on \mathcal{S} , and M is the uniform bound on functions in \mathcal{H} . The probability and expectation in (68) are taken with respect to \mathcal{D} . The original Pollard bound is given for $\mathbb{F} = \mathbb{R}$. A rederivation shows that it equally applies to $\mathbb{F} = \mathbb{C}$. Compared with the argument in [36], the Pollard bound exploits the covering number in a more subtle way.

In this paper, the function class of interest is defined as follows

$$\mathcal{H}_s = \{h(\mathbf{z}) = |\mathbf{z}^T \mathbf{h}|^2 : \mathbf{h} \in \mathbb{R}^n, \|\mathbf{h}\|_2 = 1, \|\mathbf{h}\|_1 \leq s\}. \quad (69)$$

Here, for the Bernoulli ensemble, the domain \mathcal{B} of each function $h \in \mathcal{H}_s$ is the set of binary vectors whose components assume only $+1$ and -1 , namely, $\mathcal{B} = \{+1, -1\}^n$. For the Fourier ensemble, $\mathcal{B} = \{W_0, \dots, W_{n-1}\}$. It is easy to see that \mathcal{H}_s is a bounded function class defined on \mathcal{B} in both cases as

$$|\mathbf{z}^T \mathbf{h}| \leq \sum_{\alpha=1}^n |\mathbf{z}^\alpha| |\mathbf{h}^\alpha| \leq \sum_{\alpha=1}^n |\mathbf{h}^\alpha| \leq s. \quad (70)$$

As a consequence, we obtain

$$\sup_{h \in \mathcal{H}_s, \mathbf{z} \in \mathcal{B}} |h(\mathbf{z})| \leq s^2. \quad (71)$$

Now we are ready to prove Theorem 4:

Proof: Consider a distribution \mathcal{D} on \mathcal{B} , and let $Z_1^m = \{z_1, \dots, z_m\} \subseteq \mathcal{B}$ be m independent samples from \mathcal{D} . The distributions \mathcal{D} of interest are the equal probability Bernoulli distribution, that is,

$$\mathbb{P}_{\mathcal{D}}(z_{\alpha}^{\beta} = 1) = \mathbb{P}_{\mathcal{D}}(z_{\alpha}^{\beta} = -1) = 1/2, \quad (72)$$

and the selection with replacement distribution:

$$\mathbb{P}_{\mathcal{D}}\{z_{\alpha} = W_{\beta}\} = \frac{1}{n}, \quad \beta = 0, \dots, n-1; \quad \alpha = 1, \dots, m, \quad (73)$$

for the Bernoulli ensemble and modified Fourier ensemble, respectively. Then, Pollard's bound states that for any $m \geq 1$ and $\epsilon > 0$

$$\begin{aligned} & \mathbb{P}_{\mathcal{D}} \left[\sup_{h \in \mathcal{H}_s} \left| \frac{1}{m} \sum_{i=1}^m h(z_i) - \mathbb{E}_{\mathcal{D}} h(\mathbf{z}) \right| > \epsilon \right] \\ & \leq 8 \mathbb{E}_{\mathcal{D}} \left[N \left(\frac{\epsilon}{8}, \mathcal{H}_s(Z_1^m), d_1 \right) \right] \exp \left(-\frac{m\epsilon^2}{128s^4} \right). \end{aligned} \quad (74)$$

To see the connection of (74) with ℓ_1 -CMSVs, it is observed that both the Bernoulli and Fourier sensing matrices can be equivalently written as

$$A = \frac{1}{\sqrt{m}} [z_1, \dots, z_m]^T \in \mathbb{F}^{m \times n}, \quad (75)$$

with z_i following *i.i.d.* distributions specified by (72) and (73), respectively. Note that

$$\|A\mathbf{h}\|_2^2 = \frac{1}{m} \sum_{\alpha=1}^m |z_{\alpha}^T \mathbf{h}|^2 = \frac{1}{m} \sum_{\alpha=1}^m h(z_{\alpha}). \quad (76)$$

In addition, $\|\mathbf{h}\|_2 = 1$ yields

$$\begin{aligned} \mathbb{E}_{\mathcal{D}} h(\mathbf{z}) &= \mathbb{E}_{\mathcal{D}} \sum_{\alpha, \beta=1}^n \mathbf{h}^{\alpha} \mathbf{h}^{\beta} z^{\alpha} (z^{\beta})^{\dagger} \\ &= \sum_{\alpha=1}^n (\mathbf{h}^{\alpha})^2 \mathbb{E}_{\mathcal{D}} |z^{\alpha}|^2 \\ &= \|\mathbf{h}\|_2^2 = 1, \end{aligned} \quad (77)$$

where \dagger denotes the complex conjugate. It is easy to understand the derivation leading to (77) for Bernoulli matrices. For Fourier matrices, it follows from

$$\begin{aligned}\mathbb{E}_{\mathcal{D}} z^\alpha (z^\beta)^\dagger &= \mathbb{E}_{\mathcal{D}} \left(W_l^\alpha (W_l^\beta)^\dagger \right) \\ &= \frac{1}{n} \sum_{l=0}^{n-1} e^{-j \frac{2\pi l(\alpha-\beta)}{n}} \\ &= \begin{cases} 0, & \text{if } \alpha \neq \beta; \\ 1, & \text{if } \alpha = \beta. \end{cases}\end{aligned}\quad (78)$$

If (74) is valid for a small right hand side, then with high probability the following holds:

$$\sup_{\mathbf{h}: \|\mathbf{h}\|_2=1, \|\mathbf{h}\|_1 \leq s} \left| \|\mathbf{A}\mathbf{h}\|_2^2 - 1 \right| \leq \epsilon. \quad (79)$$

As a consequence, the ℓ_1 -constrained minimal and maximal singular values of A satisfy

$$1 - \epsilon \leq (\rho_s^{\min})^2 \leq (\rho_s^{\max})^2 \leq 1 + \epsilon. \quad (80)$$

The key now is calculating the covering number $N(\epsilon, \mathcal{H}_s(Z_1^m), d_1)$. Our results rely on the covering number bounds of regularized linear function classes [44], as given in Lemma 1 following this proof. The bound (87), which is a corollary of Lemma 1, yields

$$\begin{aligned}& \mathbb{P}_{\mathcal{D}} \left[\sup_{\mathbf{h} \in \mathcal{H}} \left| \|\mathbf{A}\mathbf{h}\|_2^2 - 1 \right| > \epsilon \right] \\ & \leq 8(2n+1)^{\lceil 256s^4/\epsilon^2 \rceil} \exp\left(-\frac{m\epsilon^2}{128s^4}\right) \\ & = 8 \exp\left(-\frac{m\epsilon^2}{128s^4} + \lceil \frac{256s^4}{\epsilon^2} \rceil \log(2n+1)\right).\end{aligned}\quad (81)$$

The requirement $m\epsilon^2/(128s^4) \geq 2 \cdot \lceil 256s^4/\epsilon^2 \rceil \log(2n+1)$, which guarantees a vanishing right hand side of (81), leads to the following sufficient condition

$$m \geq c(\epsilon)s^8 \log n \quad (82)$$

for some suitably selected constant $c(\epsilon)$ depending only on ϵ . ■

Lemma 1 gives a bound on the covering number of general regularized linear function classes [44]:

Lemma 1 Denote by $\mathcal{L}_{p,q}^{a,b}$ the regularized linear function class $\{f(\mathbf{z}) = \mathbf{z}^T \mathbf{f} : \|\mathbf{f}\|_q \leq a\}$, where the domain for each $f(\cdot)$ is contained in $\{\mathbf{z} : \|\mathbf{z}\|_p \leq b\}$. Here $1/p + 1/q = 1$ and $2 \leq p \leq \infty$. Then we have

$$N(\epsilon, \mathcal{L}_{p,q}^{a,b}(Z_1^m), d_2) \leq (2n+1)^{\lceil a^2 b^2 / \epsilon^2 \rceil}, \quad (83)$$

where $d_2(\mathbf{x}, \mathbf{y}) = \frac{1}{\sqrt{m}} \|\mathbf{x} - \mathbf{y}\|_2$, $Z_1^m = \{\mathbf{z}_1, \dots, \mathbf{z}_m\}$ and $\lceil x \rceil$ is the smallest integer not less than x .

To apply Lemma 1, consider $\mathcal{L}_{\infty,1}(s, 1)$ and note that

$$\begin{aligned} & N(\epsilon, \mathcal{L}_{\infty,1}^{s,1}(Z_1^m), d_1) \\ & \leq N(\epsilon, \mathcal{L}_{\infty,1}^{s,1}(Z_1^m), d_2) \\ & \leq (2n+1)^{\lceil s^2 / \epsilon^2 \rceil}. \end{aligned} \quad (84)$$

Suppose $\{\mathbf{c}_\beta\}$ defines a ϵ -cover for $\mathcal{L}_{\infty,1}^{s,1}(Z_1^m)$ under d_1 that achieves the covering number.

Then, for any $\mathbf{h} \in \mathbb{R}^n$ with $\|\mathbf{h}\|_1 \leq s$, there exists \mathbf{c}_β such that

$$d_1(f_{\mathbf{h}}(Z_1^m), \mathbf{c}_\beta) = \frac{1}{m} \sum_{\alpha=1}^m |\mathbf{z}_\alpha^T \mathbf{h} - \mathbf{c}_\beta^\alpha| \leq \epsilon, \quad (85)$$

where $f_{\mathbf{h}}(Z_1^m) \stackrel{\text{def}}{=} (\mathbf{z}_1^T \mathbf{h}, \dots, \mathbf{z}_m^T \mathbf{h}) \in \mathbb{F}^m$. Therefore, we have

$$\begin{aligned} d_1(h(Z_1^m), \mathbf{c}_\beta) &= \frac{1}{m} \sum_{\alpha=1}^m \left| |\mathbf{z}_\alpha^T \mathbf{h}|^2 - |\mathbf{c}_\beta^\alpha|^2 \right| \\ &\leq \frac{1}{m} \sum_{\alpha=1}^m |\mathbf{z}_\alpha^T \mathbf{h} - \mathbf{c}_\beta^\alpha| |\mathbf{z}_\alpha^T \mathbf{h} + \mathbf{c}_\beta^\alpha| \\ &\leq 2s\epsilon. \end{aligned} \quad (86)$$

Consequently, the set $\{|\mathbf{c}_\beta|^2\}$, where the operation $|\cdot|^2$ is elementwise, forms a $2s\epsilon$ -cover for $\mathcal{H}_s(Z_1^m)$ under d_1 and

$$\mathcal{N}(\epsilon, \mathcal{H}_s(Z_1^m), d_1) \leq (2n+1)^{\lceil 4s^4 / \epsilon^2 \rceil}. \quad (87)$$

One limitation of the proof is the boundedness assumption of the function class \mathcal{H}_s . The boundedness of \mathcal{H}_s for the Bernoulli ensemble and modified Fourier ensemble, *i.e.*, equation (71), is obtained by restricting to their domain \mathcal{B} . However, for the Gaussian ensemble, the domain of functions in \mathcal{H}_s is the entire \mathbb{R}^n . Hence, boundedness is not guaranteed.

The covering number bound could be improved, which would lead to an overall improvement of Theorem 4. In applying Lemma 1, the set $\{f_{\mathbf{h}}(Z_1^m) : \|\mathbf{h}\|_1 \leq s\}$ is covered instead of $\{f_{\mathbf{h}}(Z_1^m) : \|\mathbf{h}\|_1 \leq s, \|\mathbf{h}\|_2 = 1\}$. The latter set might be significantly smaller than the former and can be covered with ϵ precision using significantly fewer points.

V. COMPUTATION OF THE ℓ_1 -CONSTRAINED SINGULAR VALUES

One major advantage of using the ℓ_1 -CMSV as a measure of the "goodness" of a sensing matrix is the relative ease of its computation. We show in this section that ρ_s^{\min} and ρ_s^{\max} are computationally more amenable than δ_k , whose computation involves ν_k^{\min} and ν_k^{\max} . The discrete nature of the definition of k -sparse singular values makes the algorithm design for computing them very difficult. For example, in order to compute ν_k^{\min} , the following optimization problem, which involves an ℓ_0 constraint, must be solved

$$\begin{aligned} & \min_{\mathbf{x} \in \mathbb{R}^n} \|A\mathbf{x}\|_2 \\ & \text{subject to} \\ & \|\mathbf{x}\|_0 \leq k, \end{aligned} \tag{88}$$

$$\|\mathbf{x}\|_2 = 1. \tag{89}$$

As in (2), it is might be tempting to replace the ℓ_0 constraint with $\|\mathbf{x}\|_1 \leq k$. However, a better relaxation, $\|\mathbf{x}\|_1 \leq \sqrt{k}$, is obtained by considering the second ℓ_2 constraint (89) and Schwartz inequality. Therefore, the relaxed optimization problem is

$$\min_{\mathbf{x} \in \mathbb{R}^n} \|A\mathbf{x}\|_2 \quad \text{subject to} \quad \|\mathbf{x}\|_1 \leq \sqrt{k}, \quad \|\mathbf{x}\|_2 = 1, \tag{90}$$

whose optimal value is exactly $\rho_{\sqrt{k}}^{\min}$. Unfortunately, the resulting optimization is not convex because of the ℓ_2 constraint $\|\mathbf{x}\|_2 = 1$. However, many tools at our disposal can deal with the continuous problem (90), for example, the Lagrange multiplier or the Karush-Kuhn-Tucker condition [45]. In the following subsections, we will present three algorithms to directly compute an approximate numerical solution of (90). Since the optimization problem (90) is not convex, there is no guarantee that the solutions of these algorithms are the true minima. We will also present a convex program to compute a lower bound on ℓ_1 -CMSV.

A. Projected gradient method

The projected gradient (PG) method is a continuous time approach to solve optimization problems with equality constraints. Consider the minimization of an objective function $F(\mathbf{z})$. The usual descent gradient method is equivalent to the following gradient flow [33], [46]:

$$\frac{d\mathbf{z}(t)}{dt} = -\nabla F(\mathbf{z}(t)). \quad (91)$$

When there is an equality constraint $G(\mathbf{z}) = 0$, the solution of the corresponding constrained optimization problem

$$\min_{\mathbf{z}} F(\mathbf{z}) \quad \text{subject to} \quad G(\mathbf{z}) = 0 \quad (92)$$

must lie on the manifold $M \stackrel{\text{def}}{=} \{\mathbf{z} : G(\mathbf{z}) = 0\}$. The projected gradient method directs the flow $\mathbf{z}(t)$ onto the manifold by projecting the gradient vector $\nabla F(\mathbf{z}(t))$ onto M 's tangent space:

$$\frac{d\mathbf{z}(t)}{dt} = -\pi(\nabla F(\mathbf{z}(t))), \quad (93)$$

where $\pi(\cdot)$ is the projection operator of the tangent space M .

Trendafilov and Jolliffe used the projected gradient method to compute principal components subject to a ℓ_1 type constraint, a problem termed the Simplified Component Technique-LASSO (SCoTLASS) [33]. The ℓ_1 constraint enforces the sparsity of the resulting principal components, hence facilitating extraction and interpretation [47]. Therefore, SCoTLASS falls into the category of sparse principal component analysis. The algorithm used in this paper is essentially the same as the one in [33] except that we are most interested in computing the minimal singular value.

In order to incorporate the ℓ_1 constraint, which is an inequality constraint, into the objective function, it is necessary to introduce an exterior penalty function. Consider the following optimization problem to obtain the ℓ_1 -CMSV:

$$\min_{\mathbf{z} \in \mathbb{R}^n} \mathbf{z}^T A^T A \mathbf{z} \quad \text{subject to} \quad \|\mathbf{z}\|_1 \leq s, \quad \|\mathbf{z}\|_2 = 1. \quad (94)$$

A well-known exterior penalty function for maintaining the inequality constraint is the Zangwill function, $P(\|\mathbf{z}\|_1 - s) = \max(0, \|\mathbf{z}\|_1 - s)$. The Zangwill function induces a positive penalty proportional to the violation of the constraint $\|\mathbf{z}\|_1 \leq s$ and zero penalty otherwise. Unfortunately, both the max operation and the ℓ_1 norm are discontinuous functions. Two continuous functions are employed to approximate them as suggested by [33]. First, note that $\|\mathbf{z}\|_1 = \mathbf{z}^T \text{sign}(\mathbf{z})$, where $\text{sign}(\cdot)$ denotes the elementwise sign of a vector. Then, the sign function is approximated using

$\tanh(\gamma z)$ for large γ (e.g., $\gamma = 1000$). Second, the Zangwill penalty function $P(x) = \max(0, x)$ is approximated by

$$\tilde{P}(x) = 0.5x(1 + \tanh(\gamma x)). \quad (95)$$

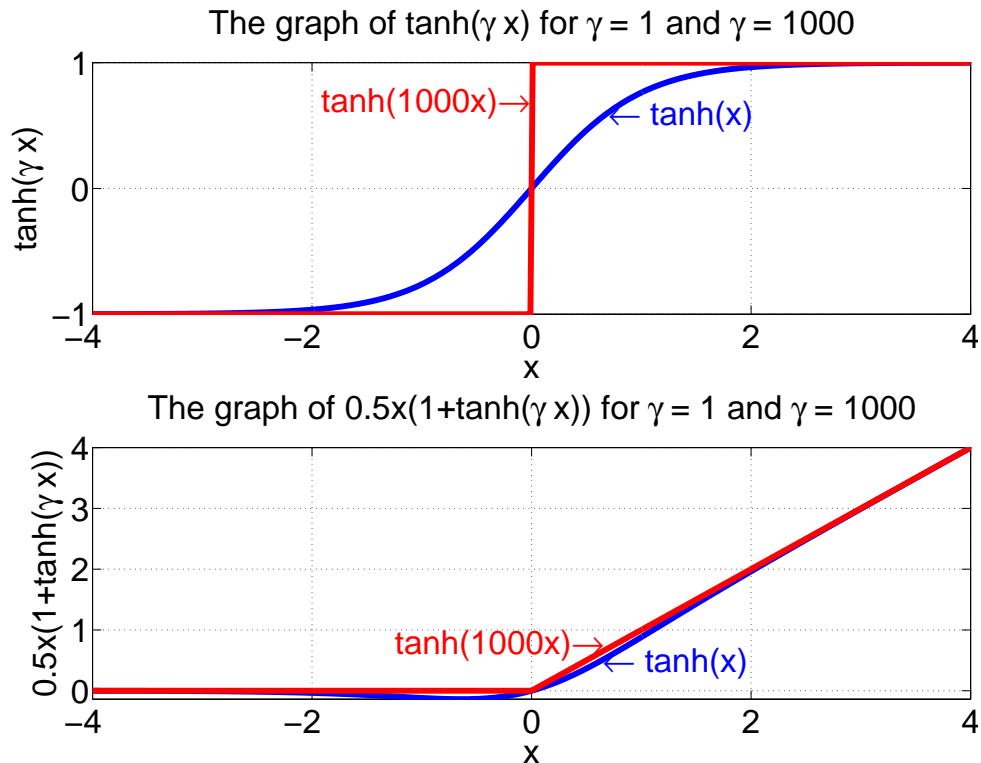


Fig. 4: The approximations of the sign function and the Zangwill penalty function

These two approximation functions are plotted in Figure 4, which replicates of Figure 1 and part of Figure 2 in [33]. Finally, the following new penalized objective function is defined:

$$F_\mu(z) = z^T A^T A z + \mu \tilde{P}(z^T \tanh(\gamma z) - s), \quad (96)$$

where $\mu > 0$, e.g., $\mu = 10$.

We formulate the projected gradient method for solving (94) based on the two approximations. The gradient vector $\nabla F_\mu(z)$ in (93) is given by

$$\nabla_{F_\mu} = 2A^T A z + 0.5\mu [1 + \tanh(\gamma \eta) + \cosh^{-2}(\gamma \eta)] \xi, \quad (97)$$

where

$$\eta = \mathbf{z}^T \tanh(\gamma \mathbf{z}) - s \quad (98)$$

and

$$\boldsymbol{\xi} = \tanh(\gamma \mathbf{z}) + \cosh^{-2}(\gamma \mathbf{z}) \odot (\gamma \mathbf{z}). \quad (99)$$

Here \odot denotes elementwise multiplication. Equation (97), together with the projection $\pi = \mathbf{I}_n - \mathbf{z}\mathbf{z}^T$, defines a complete vector dynamical system:

$$\text{PG: } \frac{d\mathbf{z}(t)}{dt} = -\pi(\nabla F_\mu(\mathbf{z}(t))). \quad (100)$$

The flow $\mathbf{z}(t)$ converges to an approximate minimum of (94).

B. Interior point method

The interior point (IP) method provides a general approach to efficiently solve the following general constrained optimization problem:

$$\min_{\mathbf{z} \in \mathbb{R}^n} F(\mathbf{z}) \quad \text{subject to } f(\mathbf{z}) \leq 0, \quad g(\mathbf{z}) = 0. \quad (101)$$

The basic idea is to construct and solve a sequence of penalized optimization problems with equality constraints:

$$\begin{aligned} \min_{\mathbf{z}, \sigma} F(\mathbf{z}) - \mu \sum_i \log(\sigma_i) \\ \text{subject to } f(\mathbf{z}) + \sigma = 0 \text{ and } g(\mathbf{z}) = 0. \end{aligned} \quad (102)$$

By using either a Newton step, which tries to solve the Karush-Kuhn-Tucker equations [45], or a conjugate gradient step using trust regions to solve the penalized problem (102) in each iteration, the interior point approach efficiently generates a sequence of solutions that converge to the solution of (101). This approach is described in [48] [49] [50] and implemented by the interior point algorithm of the MATLAB[®] function *fmincon* of the Optimization Toolbox [51].

However, the interior point approach assumes objective and constraint functions with continuous second order derivatives, which is not satisfied by the constraint $\|\mathbf{z}\|_1 - s \leq 0$. Our numerical simulation shows that the interior point algorithm exhibits instability if this issue is not taken care of. Two approaches will be employed to address the non-differentiability of $f(\mathbf{z}) = \|\mathbf{z}\|_1 - s$. The first approach uses $\tilde{f}(\mathbf{z}) = \mathbf{z}^T \tanh(\gamma \mathbf{z}) - s$ for large γ to approximate

$f(\mathbf{z})$, as done for the projected gradient method. Therefore, the non-differentiable optimization (94) is transformed to the following differentiable constrained nonlinear optimization problem:

$$\begin{aligned} \text{IP I: } & \min_{\mathbf{z} \in \mathbb{R}^n} \mathbf{z}^T A^T A \mathbf{z} \\ & \text{subject to } \mathbf{z}^T \tanh(\gamma \mathbf{z}) - s \leq 0, \quad \mathbf{z}^T \mathbf{z} = 1. \end{aligned} \quad (103)$$

The second approach defines $\mathbf{z} = \mathbf{z}^+ - \mathbf{z}^-$ with $\mathbf{z}^+ = \max(\mathbf{z}, \mathbf{0}) \geq 0$ and $\mathbf{z}^- = \max(-\mathbf{z}, \mathbf{0}) \geq 0$, which leads to the following augmented optimization:

$$\begin{aligned} \text{IP II: } & \min_{\mathbf{z}^+, \mathbf{z}^- \in \mathbb{R}^n} (\mathbf{z}^+ - \mathbf{z}^-)^T A^T A (\mathbf{z}^+ - \mathbf{z}^-) \\ & \text{subject to } \sum_i z_i^+ + \sum_i z_i^- - s \leq 0, \\ & (\mathbf{z}^+ - \mathbf{z}^-)^T (\mathbf{z}^+ - \mathbf{z}^-) = 1, \\ & \mathbf{z}^+ \geq 0, \quad \mathbf{z}^- \geq 0. \end{aligned} \quad (104)$$

Note that one additional constraint

$$\sum_i z_i^+ z_i^- = 0, \quad (105)$$

would define a one-to-one correspondence between the feasible set of the augmented problem (104) and the feasible set of (94), because constraint (105), together with the nonnegativity constraints, necessitates at most one positive element between z_i^+ and z_i^- . However, the highly nonlinearity of (105) would reduce the speed, accuracy, and stability of the corresponding interior point algorithm. Therefore, we use the augmented problem (104) without (105).

C. Lifting procedure for bounds computation

We briefly describe a semidefinite relaxation (SDR) scheme to compute a lower bound on ℓ_1 -CMSV. A similar approach was employed in [30] to compute an upper bound on sparse variance maximization using the *lifting procedure* for semidefinite programming [52]–[54]. Defining $Z =$

$\mathbf{z}^T \mathbf{z}$ transforms problem (94) into the following equivalent form:

$$\begin{aligned}
& \max_{Z \in \mathbb{R}^{n \times n}} && \text{trace}(A^T AZ) \\
\text{subject to} &&& \mathbf{1}^T |Z| \mathbf{1} \leq s^2, \\
&&& \text{trace}(Z) = 1, \\
&&& Z \succeq 0, \\
&&& \text{rank}(Z) = 1.
\end{aligned} \tag{106}$$

The *lifting procedure* relaxes the problem (106) by dropping the $\text{rank}(Z) = 1$ constraint:

$$\begin{aligned}
\text{SDR: } & \max_{Z \in \mathbb{R}^{n \times n}} && \text{trace}(A^T AZ) \\
& \text{subject to} && \mathbf{1}^T |Z| \mathbf{1} \leq s^2, \\
&&& \text{trace}(Z) = 1, \\
&&& Z \succeq 0.
\end{aligned} \tag{107}$$

Now SDR is a semidefinite programming problem. For a small size problem, a global minimum can be achieved at high precision using SEDUMI [55], SDPT3 [56] or CVX [57]. However, for relatively large n , the interior point algorithm makes the memory requirement prohibitive (see [30] for more discussion). Although the first order algorithm used in [30] can be adapted to solve a penalized version of SDR, it does not give a direct solution to SDR with fixed s .

VI. NUMERICAL SIMULATIONS

We use numerical simulations to assess the effectiveness and efficiency of the four algorithms presented in Section V. We first briefly describe the implementation details of the algorithms. Then, we illustrate the numerical precision and running time for small-scale and medium-scale problems. In the last subsection, we present the ℓ_1 -CMSVs computed for various values of m , n , and s .

We provide implementation details for the projected gradient algorithm PG, two interior point algorithms IP I and IP II, as well as the semidefinite relaxation algorithm SDR. For the projected gradient algorithm, MATLAB[®] function *ode15s* is used with relative error tolerance (*'RelTol'*) and absolute error tolerance (*'AbsTol'*) set to 10^{-8} . The adjustable parameters are set to $\mu = 10$ and $\gamma = 10^5$ in (96). The two interior point algorithms IP I and IP II are implemented using

the MATLAB[®] function *fmincon*, a general procedure for finding a minimum of a constrained nonlinear multivariate function. The ‘*Algorithm*’ option for *fmincon* is set to ‘*interior-point*’. For better global convergence, the parameter γ is increased from 1 to 10^3 , and then 10^5 for IP I. The solution from the previous γ value is fed to the later (and larger) γ value as the initial solution. To speed IP I and IP II, self-defined gradient functions for both the objective function and the constraint functions are provided to *fmincon*. The Hessian multiplication function is also defined for IP II. The SDR is solved using CVX [57] with the default SDPT3 solver.

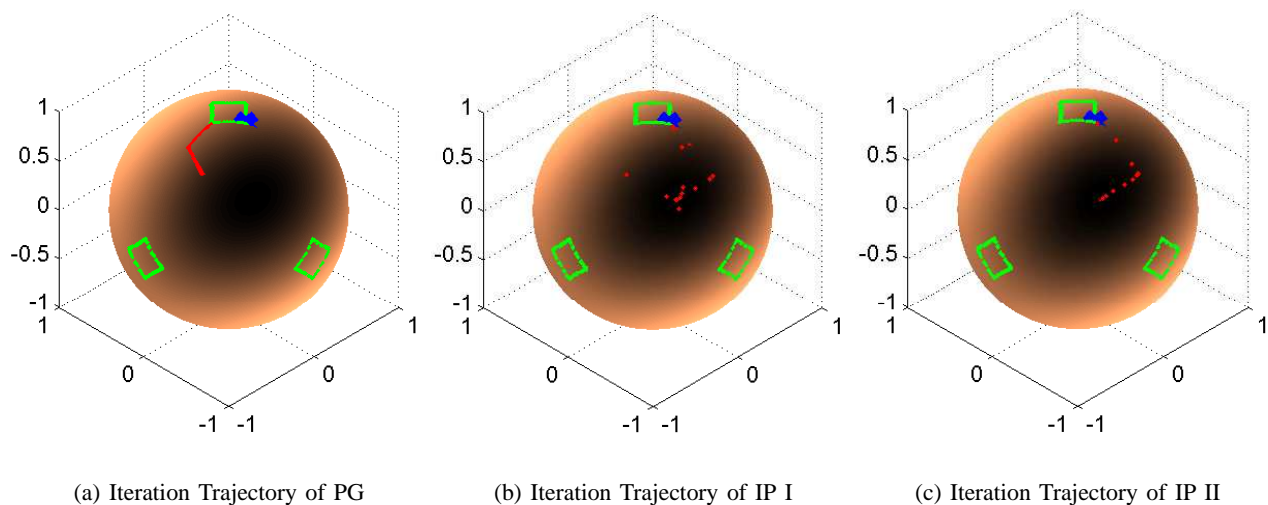


Fig. 5: Iteration Trajectory of Three Algorithms:

Figure 5 shows the iteration trajectories of the three algorithms PG, IP I and IP II for a randomly generated Gaussian matrix $A \in \mathbb{R}^{2 \times 3}$ and initial point x_0 :

$$A = \begin{bmatrix} 0.4893 & -1.7730 & -1.5438 \\ -1.5789 & 0.0996 & -0.8380 \end{bmatrix}, \text{ and}$$

$$x_0 = \begin{bmatrix} -0.5699 & -0.2601 & 0.7794 \end{bmatrix}^T.$$

The unit spheres are colored according to the value of the objective function $F(z) = z^T A^T A z$, with dark colors representing smaller values. The ℓ_1 -sparsity level is set as $s = \sqrt{1.4} \approx 1.1832$. The regions enclosed by the green semi-rectangles are points on the unit sphere that satisfy the

constraint $\|z\|_1 \leq s$. There are two global minima:

$$z_1^* \approx [0, -0.2043, 0.9789]^T, \quad \text{and} \quad (108)$$

$$z_2^* \approx [0, 0.2043, -0.9789]^T \quad (109)$$

with

$$F(z_1^*) = F(z_2^*) \approx 2.0270. \quad (110)$$

The iteration sequences of PG and IP I, shown in red, converge to z_1^* , while that of IP II converges to z_2^* . In Figure 5, the minima of $F(z)$ under the ℓ_1 constraint are shown in blue, although the minimum z_2^* is on the back surface of the sphere. For better comparison, the signs of the iteration sequence of IP II are flipped for display in Figure 5c. Multiple runs of this simple example with Gaussian matrices in $\mathbb{R}^{2 \times 3}$ demonstrate that IP I and IP II have better global convergence, while PG sometimes produces non-global minima.

The four algorithms PG, IP I, IP II, and SDR are tested for small-scale problems with a Gaussian matrix $A \in \mathbb{R}^{20 \times 60}$ and ℓ_1 -sparsity level $s = \sqrt{5} \approx 2.2361$. $T = 50$ initial points on the unit sphere in \mathbb{R}^{60} are randomly generated for PG, IP I and IP II. Those initial points do not necessarily satisfy the constraint $\|z\|_1 \leq s$. The function values $F(z^*)$, the running times, and the ℓ_1 and ℓ_2 norms of the final solutions z^* are recorded for each initial point. Because it is not necessary to provide an initial point for SDR, it is run only once, and the corresponding quantities are recorded. We remark that, due to the existence of local minima, in practice we need to run PG, IP I or IP II several times and select the minimal function value among all trials as the ℓ_1 -CMSV, a strategy used to prepare Figures 8 and 9.

TABLE I: Comparison of different characteristics of PG, IP I, IP II, and SDR for $A \in \mathbb{R}^{20 \times 60}$

	$\min F(z^*)$	$\text{mean}F(z^*)$	$\text{std}F(z^*)$	mean time (sec.)	time std/mean
PG	0.0664 ✓	1.2197	0.6924	5.1079	23.99% ✓
IP I	0.0674	0.9941	0.5225	6.7313	44.36%
IP II	0.0666	0.7133 ✓	0.3661 ✓	2.8903 ✓	34.13%
SDR	0.0000	0.0000	N/A	53.1583	N/A

The results are presented in Figure 6 and Table I. Figure 6a and the second column of Table I show that the three non-convex algorithms PG, IP I, and IP II produce almost the same minimal

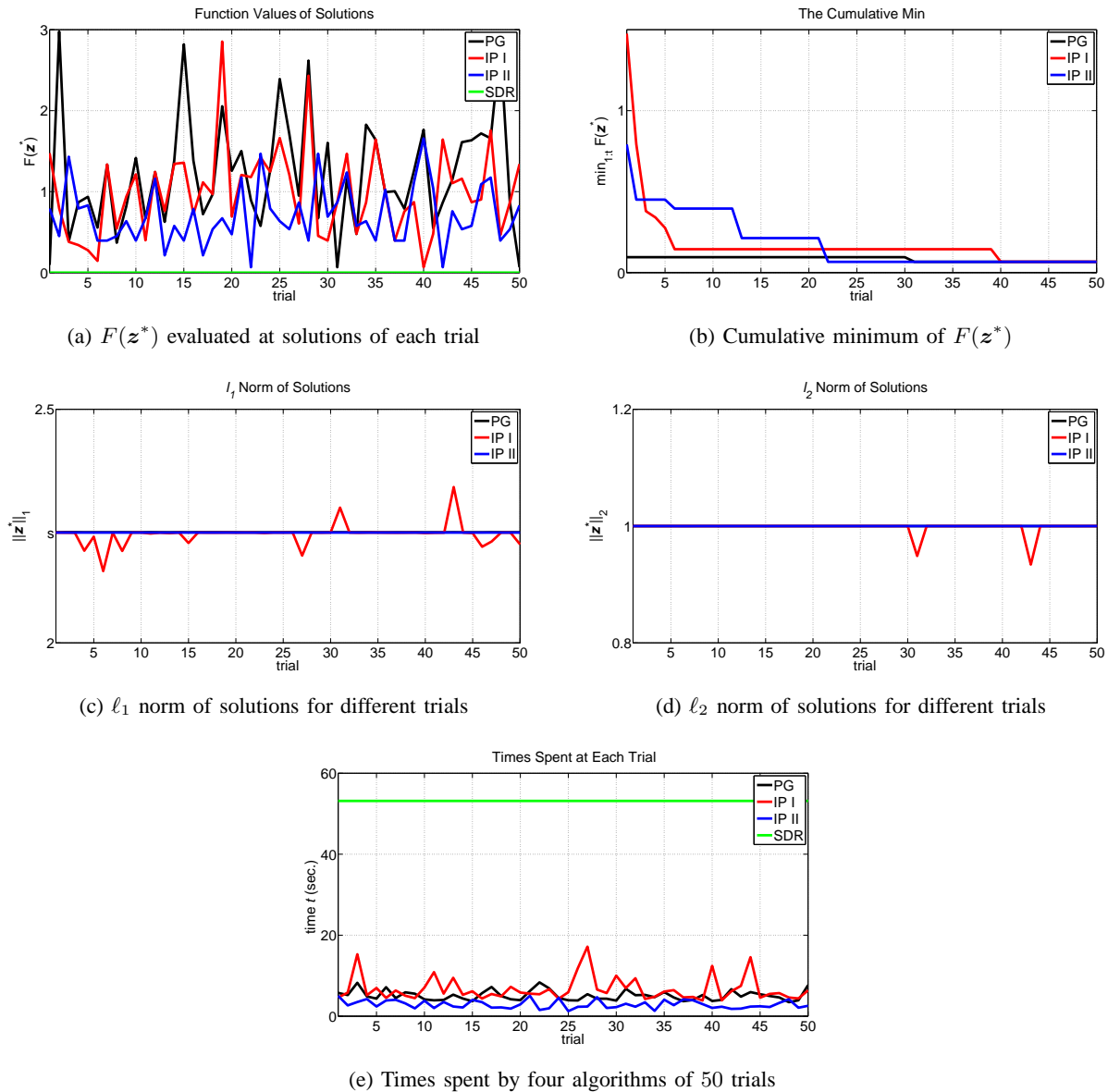


Fig. 6: Results of PG, IP I, IP II, and SDR for a Gaussian matrix $A \in \mathbb{R}^{20 \times 60}$ with 50 different random initial points.

values of $F(z)$. The PG algorithm may seem a little bit better, but zooming in on Figure 6c shows that the ℓ_1 norms of its solutions are actually a little bit higher than $s = \sqrt{5}$ due to the approximation of the ℓ_1 norm. For this particular realization of A , SDR over-relaxes the problem and gives a zero bound on the ℓ_1 -CMSV. As far as the running times are concerned, the IP II algorithm performs significantly better than all other algorithms. The SDR algorithm is the most

TABLE II: Comparison of different characteristics of PG, IP I and IP II for a Bernoulli matrix $A \in \mathbb{R}^{50 \times 500}$

	$\min F(\mathbf{z}^*)$	$\text{mean}F(\mathbf{z}^*)$	$\text{std}F(\mathbf{z}^*)$	mean time (sec.)	time std/mean
PG	0.020848	0.057152	0.029494	886.3322	26.42% ✓
IP I	0.003608	0.025381	0.017350	293.7871	46.65%
IP II	0.000371 ✓	0.007472 ✓	0.004545 ✓	123.6456 ✓	82.05%

time-consuming as well as memory-consuming. In fact, when $n \geq 80$ (this value might depend on the CVX version and computer), the CVX implemented SDR takes so much memory that it can not be run in MATLAB[®]. Therefore, for a medium-scale problem with $n = 500$, only the three non-convex algorithms will be tested. Figure 6b shows that IP II reaches its minimal function value earliest, which indicates that IP II has a better global convergence property. It is also found that the IP I is not very stable, in the sense that the ℓ_1 and ℓ_2 norms of final solutions sometimes violate their constraints. In each column of Table I, we use ✓ to denote the best algorithm as far as the quality corresponding to that column is concerned. Extensive testing confirms our observation that IP II is the most accurate and stable algorithm for small-scale problems.

The three non-convex algorithms, PG, IP I and IP II, are also tested for a medium-scale Bernoulli matrix $A \in \mathbb{R}^{50 \times 500}$. The results are shown in Figure 7 and Table II. As mentioned previously, the SDR takes too much memory to run for $n = 500$. The simulation setup is the same as the case for $n = 60$. Figure 7 and Table II further confirm that IP II is the most accurate and stable algorithm. As the dimension increases, PG tends to be trapped in local minima, as shown in Figure 7a and 7b. The execution time of algorithm PG also increases dramatically (Figure 7e and the fourth column of Table II). Furthermore, Figure 7c and 7d demonstrate that the algorithm IP I becomes increasingly unstable, with more violations of ℓ_1 and ℓ_2 constraints. For these reasons, we will use multiple runs of the IP II algorithm to compute the ℓ_1 -CMSVs for varying n, m , and s .

We compare the ℓ_1 -CMSVs ρ_s and their bounds as a function of s computed by IP II and SDR, respectively, for Bernoulli random matrices. First, we consider a small-scale problem with $n = 60$ and $m = 10, 20, 40$. A matrix $B \in \mathbb{R}^{40 \times 60}$ with entries $\{+1, -1\}$ following $\frac{1}{2}$ Bernoulli

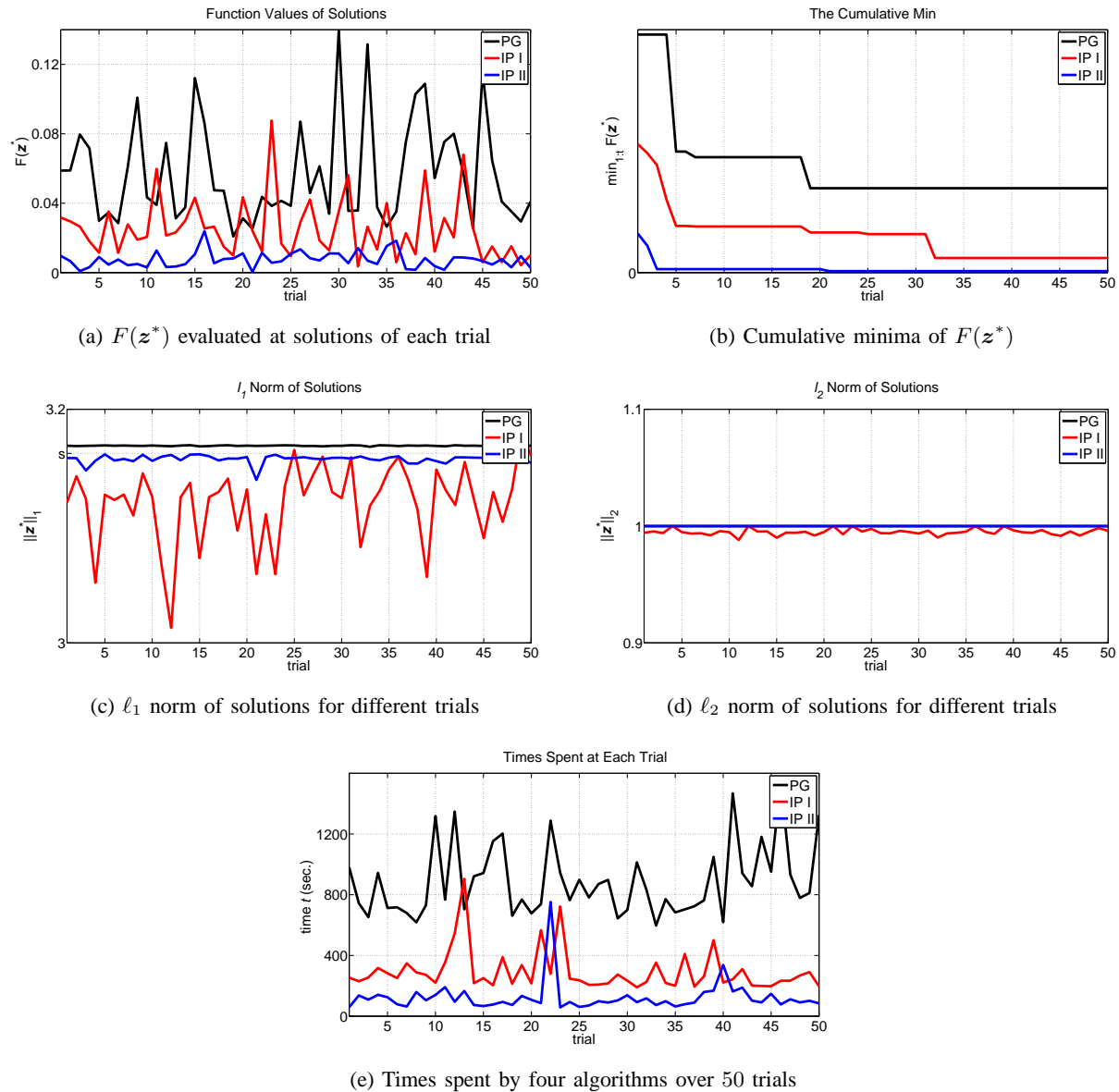


Fig. 7: Results of PG, IP I, IP II for a Bernoulli matrix $A \in \mathbb{R}^{50 \times 500}$ with 50 different random initial points.

distribution is generated. For $m = 10, 20, 40$, the corresponding Bernoulli matrix A is obtained by taking the first m rows of B . The columns of A are then normalized by multiplying $1/\sqrt{m}$. The normalization implies that $\rho_s \leq \rho_1 = 1$. For each m , the sparsity levels s are 20 uniform samples in $[1.5, \sqrt{m/2}]$. The IP II uses 30 random initial points and selects the solution with smallest function value. As illustrated in Figure 8, the ℓ_1 -CMSVs and their bounds decrease very

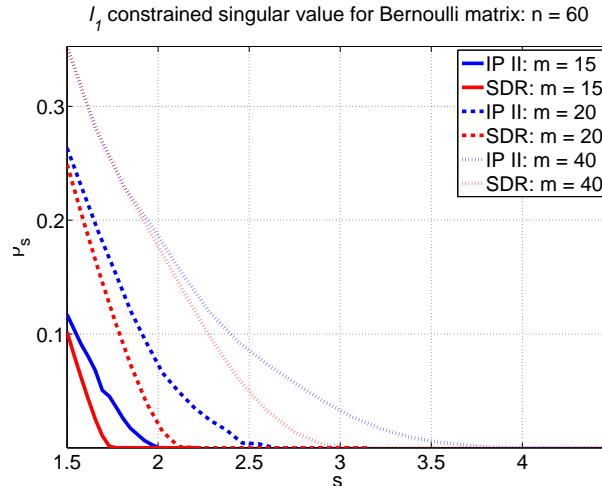


Fig. 8: ℓ_1 -CMSV ρ_s and its bound as a function of s for Bernoulli matrix with $n = 60$ and $m = 10, 20, 40$.

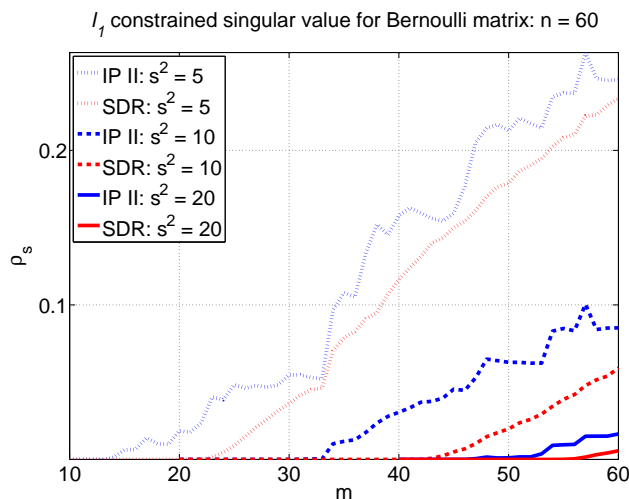


Fig. 9: ℓ_1 -CMSV ρ_s and its bound as a function of m for Bernoulli matrix with $n = 60$ and $s = \sqrt{5}, \sqrt{10}, \sqrt{20}$.

fast as s increases. For fixed s , increasing m generally (but not necessarily, as shown in Figure 9) increases the ℓ_1 -CMSV and their bounds.

In Figure 9, the ℓ_1 -CMSV ρ_s is plotted as a function of m with varying parameter values: $s = \sqrt{5}, \sqrt{10}$ and $\sqrt{20}$. As in the setup for Figure 8, we first generate a matrix $B \in \mathbb{R}^{60 \times 60}$ with entries $\{+1, -1\}$ following $\frac{1}{2}$ Bernoulli distribution. With s fixed, the two algorithms (IP

II and SDR) are run for $A \in \mathbb{R}^{m \times n}$, with m increasing from $2s^2$ to $n = 60$. For each m , the construction of A follows the procedure described in the previous paragraph. The discrete nature of adding rows to A while increasing m makes the curves in Figure 9 not as smooth as those in Figure 8. The ρ_s increases with m in general, but local decreases do happen. The gap between values computed by IP II and SDR is also clearly seen for medium s .

The extensive simulations in this section shows that IP II is the most accurate and efficient algorithm among the four. The $z = z^+ - z^-$ transformation increases the search space and avoids the highly nonlinearity of the constraint $\|z\|_1 = s$. Of course, even IP II is still by no means efficient, as it takes more than two minutes for each run when $n = 500$.

VII. CONCLUSIONS

In this paper, a new measure of a sensing matrix's incoherence, the ℓ_1 -CMSV, is proposed to quantify the stability of sparse signal reconstruction. It is demonstrated that the reconstruction errors of Basis Pursuit, the Dantzig selector, and the LASSO estimator are concisely bounded using the ℓ_1 -CMSV. A covering number argument shows that the ℓ_1 -CMSV is bounded away from zero with high probability for the Bernoulli ensemble and Fourier ensemble, as long as the number of measurements is relatively large. Three non-convex programs and one semidefinite program are presented to compute the ℓ_1 -CMSV and its lower bound, respectively. Extensive numerical simulations assess the algorithms' performance. The ℓ_1 -CMSV provides a computationally amenable measure of incoherence that can be used for optimal design.

This work is incomplete in several regards. It is unclear whether the ℓ_1 -CMSV can be used to bound the reconstruction error of iterative algorithms. The analysis of the LASSO estimator deals with only the noise-free case. The derived bound on m to guarantee ℓ_1 -CMSVs bounded away from zero for random matrices is improvable and does not apply to Gaussian matrices. More importantly, the designed algorithms have no global convergence guarantee and are inefficient for medium and large problems. Our future work will address these problems as well as the use the ℓ_1 -CMSV as a basis for designing optimal sensing matrices.

REFERENCES

- [1] E. J. Candès, J. Romberg, and T. Tao, "Robust uncertainty principles: Exact signal reconstruction from highly incomplete frequency information," *IEEE Trans. Inf. Theory*, vol. 52, no. 2, pp. 489–509, Feb. 2006.

- [2] D. L. Donoho, "Compressed sensing," *IEEE Trans. Inf. Theory*, vol. 52, no. 4, pp. 1289–1306, Apr. 2006.
- [3] E. J. Candès and T. Tao, "Decoding by linear programming," *IEEE Trans. Inf. Theory*, vol. 51, no. 12, pp. 4203–4215, Dec. 2005.
- [4] E. G. Larsson and Y. Selen, "Linear regression with a sparse parameter vector," *IEEE Trans. Signal Process.*, vol. 55, no. 2, pp. 451–460, Feb. 2007.
- [5] D. Malioutov, M. Cetin, and A. S. Willsky, "A sparse signal reconstruction perspective for source localization with sensor arrays," *IEEE Trans. Signal Process.*, vol. 53, no. 8, pp. 3010–3022, Aug. 2005.
- [6] D. Model and M. Zibulevsky, "Signal reconstruction in sensor arrays using sparse representations," *Signal Processing*, vol. 86, pp. 624–638, Mar. 2006.
- [7] D. L. Donoho and P. B. Stark, "Uncertainty principles and signal recovery," *SIAM Journal on Applied Mathematics*, vol. 49, no. 3, pp. 906–931, 1989.
- [8] M. A. Sheikh, S. Sarvotham, O. Milenkovic, and R. G. Baraniuk, "DNA array decoding from nonlinear measurements by belief propagation," in *Proc. IEEE Workshop Statistical Signal Processing (SSP 2007)*, Madison, WI, Aug. 2007, pp. 215–219.
- [9] H. Vikalo, F. Parvaresh, and B. Hassibi, "On recovery of sparse signals in compressed DNA microarrays," in *Proc. Asilomar Conf. Signals, Systems and Computers (ACSSC 2007)*, Pacific Grove, CA, Nov. 2007, pp. 693–697.
- [10] F. Parvaresh, H. Vikalo, S. Misra, and B. Hassibi, "Recovering sparse signals using sparse measurement matrices in compressed DNA microarrays," *IEEE J. Sel. Topics Signal Processing*, vol. 2, no. 3, pp. 275–285, June 2008.
- [11] H. Vikalo, F. Parvaresh, S. Misra, and B. Hassibi, "Sparse measurements, compressed sampling, and DNA microarrays," in *Proc. IEEE Int. Conf. Acoustics, Speech and Signal Processing (ICASSP 2008)*, Las Vegas, NV, Apr. 2008, pp. 581–584.
- [12] R. Baraniuk and P. Steeghs, "Compressive radar imaging," in *IEEE Radar Conference*, Apr. 2007, pp. 128–133.
- [13] M. Herman and T. Strohmer, "Compressed sensing radar," in *IEEE Radar Conference*, May 2008, pp. 1–6.
- [14] M. A. Herman and T. Strohmer, "High-resolution radar via compressed sensing," *IEEE Trans. Signal Process.*, vol. 57, no. 6, pp. 2275–2284, June 2009.
- [15] Z. Tian and G. B. Giannakis, "Compressed sensing for wideband cognitive radios," in *Proc. IEEE Int. Conf. Acoustics, Speech and Signal Processing (ICASSP 2007)*, Honolulu, HI, Apr. 2007, pp. IV–1357–IV–1360.
- [16] E. J. Candès and M. B. Wakin, "An introduction to compressive sampling," *IEEE Signal Process. Mag.*, vol. 25, no. 2, pp. 21–30, Mar. 2008.
- [17] M. Elad, "Optimized projections for compressed sensing," *IEEE Trans. Signal Process.*, vol. 55, no. 12, pp. 5695–5702, Dec. 2007.
- [18] J. M. Duarte-Carvajalino and G. Sapiro, "Learning to sense sparse signals: Simultaneous sensing matrix and sparsifying dictionary optimization," *IEEE Trans. Image Process.*, vol. 18, no. 7, pp. 1395–1408, June 2009.
- [19] J. A. Tropp and A. C. Gilbert, "Signal recovery from random measurements via orthogonal matching pursuit," *IEEE Trans. Inf. Theory*, vol. 53, no. 12, pp. 4655–4666, Dec. 2007.
- [20] D. Needell and J. A. Tropp, "CoSaMP: Iterative signal recovery from incomplete and inaccurate samples," *Appl. Comput. Harmonic Anal.*, vol. 26, no. 3, pp. 301–321, May 2009.
- [21] W. Dai and O. Milenkovic, "Subspace pursuit for compressive sensing signal reconstruction," *IEEE Trans. Inf. Theory*, vol. 55, no. 5, pp. 2230–2249, May 2009.
- [22] B. Efron, T. Hastie, I. Johnstone, and R. Tibshirani, "Least angle regression," *Ann. Statist.*, vol. 32, pp. 407–499, 2004.

- [23] S. Chen, D. L. Donoho, and M. A. Saunders, “Atomic decomposition by basis pursuit,” *SIAM J. Sci. Comp.*, vol. 20, no. 1, pp. 33–61, 1998.
- [24] E. J. Candès and T. Tao, “The Dantzig selector: Statistical estimation when p is much larger than n ,” *Ann. Statist.*, vol. 35, pp. 2313–2351, 2007.
- [25] R. Tibshirani, “Regression shrinkage and selection via lasso,” *J. Roy. Statist. Soc. Ser. B*, vol. 58, pp. 267–288.
- [26] M. Wainwright, “Information-theoretic bounds on sparsity recovery in the high-dimensional and noisy setting,” in *IEEE Int. Symp. Information Theory (ISIT 2007)*, Nice, France, June 2007, pp. 961–965.
- [27] G. Tang and A. Nehorai, “Performance analysis for sparse support recovery,” *IEEE Trans. Inf. Theory*, vol. 56, no. 3, pp. 1383–1399, Mar. 2010.
- [28] E. J. Candès, “The restricted isometry property and its implications for compressed sensing,” *Compte Rendus de l’Academie des Sciences, Paris, Serie I*, vol. 346, 2008.
- [29] A. Cohen, W. Dahmen, and R. DeVore, “Compressed sensing and best k -term approximation,” *J. Amer. Math. Soc.*, vol. 22, pp. 211–231, July 2009.
- [30] A. d’Aspremont, L. El Ghaoui, M. Jordan, and G. R. G. Lanckriet, “A direct formulation for sparse PCA using semidefinite programming,” *SIAM Review*, vol. 49, no. 3, pp. 434–448, 2007.
- [31] A. d’Aspremont and L. El Ghaoui, “Testing the nullspace property using semidefinite programming,” To appear in *Mathematical Programming*.
- [32] N. Meinshausen and B. Yu, “Lasso-type recovery of sparse representations for high-dimensional data,” *Ann. Statist.*, vol. 37, pp. 246–270, 2009.
- [33] N. T. Trendafilov and I. T. Jolliffe, “Projected gradient approach to the numerical solution of the SCoTLASS,” *Comput. Stat. Data Anal.*, vol. 50, no. 1, pp. 242–253, 2006.
- [34] M. R. Osborne, B. Presnell, and B. A. Turlach, “On the LASSO and its dual,” *J. Comput. Graph. Statist.*, vol. 9, pp. 319–337, 2000.
- [35] S. S. Chen, D. L. Donoho, and M. A. Saunders, “Atomic decomposition by basis pursuit,” *SIAM Review*, vol. 43, no. 1, pp. 129–159, 2001.
- [36] R. DeVore, R. Baraniuk, M. Davenport and M. B. Wakin, “A simple proof of the restricted isometry property for random matrices,” *Constructive Approximation*, vol. 28, no. 3, pp. 253–263, 2008.
- [37] G. Tang and A. Nehorai, “Lower bounds on mean squared error for sparse signal estimation,” in preparation.
- [38] M. Rudelson and R. Vershynin, “Sparse reconstruction by convex relaxation: Fourier and gaussian measurements,” in *Proc. 40th Conf. Inf. Sci. Syst. (CISS 2006)*, march 2006, pp. 207 –212.
- [39] M. Rudelson and R. Vershynin, “On sparse reconstruction from fourier and gaussian measurements,” Tech. Rep., Communications on Pure and Applied Mathematics, 2006.
- [40] E. J. Candès and T. Tao, “Near-optimal signal recovery from random projections: Universal encoding strategies?,” *IEEE Trans. Inf. Theory*, vol. 52, no. 12, pp. 5406–5425, dec. 2006.
- [41] D. Pollard, *Convergence of stochastic processes*, Springer-Verlag, New York, NY, 1984.
- [42] L. Devroye, L. Györfi, and G. Lugosi, *A probabilistic theory of pattern recognition*, Springer-Verlag, Mew York, NY, 1996.
- [43] V. N. Vapnik, *The Nature of Statistical Learning Theory*, Springer-Verlag, New York, NY, 2000.
- [44] T. Zhang, “Covering number bounds of certain regularized linear function classes,” *J. Mach. Learn. Res.*, vol. 2, pp. 527–550, 2002.

- [45] A. Sofer S. G. Nash, *Linear and nonlinear programming*, McGraw-Hill, New York, NY, 1996.
- [46] U. Helmke and J. B. Moore, *Optimization and dynamical systems*, Springer, London, UK, 1994.
- [47] I. T. Jolliffe, N. T. Trendafilov, and M. Uddin, “A modified principal component technique based on the lasso,” *J. Comput. Graphi. Stat.*, vol. 12, no. 3, pp. 531–547, 2003.
- [48] R. H. Byrd, J. C. Gilbert, and J. Nocedal, “A trust region method based on interior point techniques for nonlinear programming,” *Mathematical Programming*, vol. 89, no. 1, pp. 149–185, 2000.
- [49] R. H. Byrd, Mary E. Hribar, and Jorge Nocedal, “An interior point algorithm for large-scale nonlinear programming,” *SIAM Journal on Optimization*, vol. 9, no. 4, pp. 877–900, 1999.
- [50] R. A. Waltz, J. L. Morales, J. Nocedal, and D. Orban, “An interior algorithm for nonlinear optimization that combines line search and trust region steps,” *Mathematical Programming*, vol. 107, no. 3, pp. 391–408, 2006.
- [51] *Optimization Toolbox 5 User’s Guide*, MathWorks, Natick, MA, 2010.
- [52] L. Lovász and A. Schrijver, “Cones of matrices and set-functions and 0-1 optimization,” *SIAM Journal on Optimization*, vol. 1, pp. 166–190, 1991.
- [53] F. Alizadeh, “Interior point methods in semidefinite programming with applications to combinatorial optimization,” *SIAM Journal on Optimization*, vol. 5, pp. 13–51, 1995.
- [54] C. Lemaréchal and F. Oustry, “Semidefinite relaxations and Lagrangian duality with application to combinatorial optimization,” *INRIA, Rapport de recherche*, vol. 3710, 1999.
- [55] J. Sturm, “Using SEDUMI 1.0x, a MATLAB toolbox for optimization over symmetric cones,” *Optimization Methods and Software*, vol. 11, pp. 625–653, 1999.
- [56] R. H. Tutuncu, K. C. Toh, and M. J. Todd, “Solving semidefinite-quadratic-linear programs using SDPT3,” *Mathematical Programming Ser. B*, vol. 95, pp. 189–217, 2003.
- [57] M. Grant and S. Boyd, “CVX: Matlab software for disciplined convex programming (web page and software),” June 2009.